

# STABLE OXIDES ON CHARs AND IMPACT OF REACTOR MATERIALS AT HIGH TEMPERATURES

*Wei-Yin Chen\*, Shaolong Wan and Guang Shi*

Department of Chemical Engineering

Anderson Hall, P.O. Box 1848

University of Mississippi

University, MS 38677-9740

Copyright<sup>©</sup>

For publication in *Energy and Fuels*

June 27, 2006

\*Corresponding author; Tel. (662) 915-5651; Fax. (662) 915-7023

E-mail address: [cmchengs@olemiss.edu](mailto:cmchengs@olemiss.edu)

# TABLE OF CONTENTS

|   |     |
|---|-----|
| ABSTRACT . . . . .  | iii |
| INTRODUCTION . . . . .  | 1   |
| EXPERIMENTAL SECTION . . . . .  | 5   |
| Experimental Apparatus . . . . .  | 5   |
| Particle Injection Methods . . . . .  | 6   |
| Transient Kinetics and Temperature-Programmed Desorption . . . . .                        | 7   |
| Samples . . . . .   | 8   |
| Reactor Tubes and Support Materials . . . . .   | 9   |
| RESULTS AND DISCUSSION . . . . .  | 9   |
| Transient Kinetics (TK) and Temperature-Programmed Desorption (TPD)                       |     |
| <i>Devolatilization, oxidation and TK at 629°C</i> . . . . .                              | 10  |
| <i>Devolatilization, oxidation and TK at 1400°C</i> . . . . .                             | 11  |
| <i>TPD at 629°C</i> . . . . .   | 11  |
| <i>TPD at 1400°C</i> . . . . .  | 14  |
| In Search of Oxygen Source for CO Production . . . . .                                    | 14  |
| Roles of Reactor Materials. . . . .   | 16  |
| <i>Alumina tube</i> . . . . .   | 16  |
| <i>Silicon carbide tube</i> . . . . .   | 20  |
| <i>Supporting materials in tubes</i> . . . . .  | 23  |
| Suggestions on the Reactor Configuration for In-Situ Study<br>of Surface Oxides . . . . . | 25  |
| CONCLUSIONS . . . . .   | 26  |
| ACKNOWLEDGMENT . . . . .  | 26  |
| REFERENCES . . . . .  | 27  |
| TABLES . . . . .  | 32  |
| LIST OF FIGURE CAPTIONS . . . . .   | 34  |
| FIGURES . . . . .   | 36  |

## Abstract

This paper reports our first study on the deactivation of young chars in flame conditions. The quantity and strength of surface oxides on young chars are monitored *in-situ* by temperature-programmed desorption (TPD) up to 1700°C. Young chars contain more abundant surface oxides than those on old chars over a wide range of temperature. Lignite chars possess more oxides than those on chars derived from a bituminous coal. Chars oxidized at 629°C show desorption products at three distinct temperatures: 725°C, 1430°C and 1700°C. The TPD peaks around 725°C correspond to activation energies in the range of 107 to 170 kJ/mol and have been well documented in the literature. CO desorbed at around 1430°C corresponds to activation energies over 300 kJ/mol, signifying the possible roles of strongly bound oxides on the basal planes of carbon. Search of the oxygen source for the huge amount of CO production at 1700°C reveals that commonly adopted alumina tubes and support materials decompose to  $\text{Al}_2\text{O}_{(\text{g})}$  and emit notable amount of  $\text{O}_2$  at temperature above 1300°C. Moreover, alumina tube and support materials react with CO and form  $\text{CO}_2$ ; they also react with carbon and form CO and aluminum oxycarbides. SiC tube, on the other hand, is oxidized by  $\text{O}_2$ ,  $\text{CO}_2$  and  $\text{H}_2\text{O}$  and forms  $\text{SiO}_{(\text{g})}$ ,  $\text{SiO}_{2(\text{s})}$ , Si,  $\text{Si}(\text{OH})_{4(\text{g})}$  and CO above 650°C. Thus, alumina appears suitable for oxidation part of the experiments where up to 120 ppm  $\text{O}_2$  emission is acceptable at temperature at 1700°C. SiC appears acceptable for TPD, though a small amount of SiC may be oxidized by the TPD product,  $\text{CO}_2$ , at temperature above 900°C. Oxidation of SiC prior to TPD should be avoided.

Keywords: young char, surface oxide,  $\text{Al}_2\text{O}_3$ , SiC, combustion, wall reactions

## INTRODUCTION

Pulverized coal or lignite particles in a typical flame undergo a rapid release of volatiles, or devolatilization, followed by a relatively slow process of char combustion. Partly due to their distinct time domains of occurrence, coal devolatilization and char oxidation have usually been studied conveniently with separate procedures in laboratories.<sup>1</sup> Under rapid heating ( $>10^4$  °C /s such as those in pulverized coal flames) in an inert gas, most of the volatile species are driven out of the coal matrix in approximately 100 ms, leaving behind only a small amount of hydrogen that evolves slowly.<sup>1,2</sup> Chars derived from pyrolysis have been subjects of various reactivity studies including their oxidation with O<sub>2</sub> and CO<sub>2</sub>,<sup>3</sup> NO/char reaction,<sup>4</sup> and desorption of surface oxides.<sup>5</sup> To ensure that the chars under investigation are “clean,” or free from foreign species adsorbed on their surface after pyrolysis, it has been a common practice to thermally treat the chars in an inert gas at about 1000°C for about 1 to 3 hr before reactivity studies. Pulverized coal particles in typical flames, however, devolatilize at higher temperatures, 1100 to 1800°C, and burn within a much shorter time, usually a few seconds.<sup>1</sup> Questions, therefore, arise concerning the reactivities of chars derived from research laboratories truly represent those in the pulverized coal flames.

The surface of char, containing all the five major elements in the coal, C, N, S, O, and H, and various mineral species, undergoes complex chemical and physical transformations in the flame immediately after the devolatilization. Consequently, it is anticipated that the thermal history of chars, including heating rate, peak temperature, and residence time, will have profound influences on the structure and, therefore, the reactivities, of char. For instance, it was reported that CaO crystallite growth is the major cause of char deactivation.<sup>6,7</sup> It was also observed that the residual carbon samples extracted from commercial and pilot-scale coal combustion fly-ash samples have lower

oxidation reactivities and more fully developed turbostratic crystallinity.<sup>8</sup> Thermal annealing, or graphitization, of the carbon structure, at high flame temperatures has been considered the principal contributor to the decline of rate of char reaction with oxygen at temperatures above 1500°C.<sup>9,10</sup> Experimental and theoretical studies of char deactivation by thermal annealing have been active for a long time,<sup>11</sup> and it was extensively reviewed by Suuberg.<sup>5</sup>

Chen and Tang<sup>12</sup> observed that NO reduction on coal-derived chars decreases substantially and rapidly with the increasing severity of coal pyrolysis in the temperature range of 950 to 1100°C and residence time range of 0 to 2 hours in fuel rich combustion. They proposed a heterogeneous NO reduction mechanism that involves multi-functional roles of catalysts on the char surface, and carbon reactive sites. This mechanism has shown technological significance as low cost, mixed fuels can be designed for effective reburning.<sup>13</sup>

The above discussion suggests that the traditional method of measuring char reactivity based on old chars has most likely underestimated that of young chars in the pulverized coal flames. It appears there is an urgent need to enhance our understanding of char reactivity in the flame region, i.e., the chars produced from pyrolysis and combustion at flame temperatures, 1100 to 1700°C and with residence times in an order of seconds.

There have been some scattered works on the study of the reactivity of young chars. Dictor<sup>14</sup> used two-color pyrometry to determine the true temperature profiles of singly burning pulverized coal particles in a variety of oxidizing atmospheres above 1500 K with a burnout time of 20 to 140 ms. Radovic et al.<sup>6,7</sup> tested the effects of pyrolysis conditions on the reactivity of demineralized and cation-exchanged lignite and CaO dispersion, where the pyrolysis condition varied from 0.3 second to 1 hour at different temperatures. Molina et al.<sup>15</sup> examined rates of NO reduction on young chars produced

in-situ, old chars produced with a long residence time and activated carbon. Both Chen and Tang<sup>12</sup> and Molina et al. reported that young chars have an one-order-of-magnitude higher NO reduction rates than those of old chars. Recently, Garijo et al.<sup>16</sup> compared a char produced in-situ with short-residence time and that pyrolyzed for 15 min, and found that the initial NO reduction rate of the young char is about 2.7 times higher than that of the old char at 1123 K.

There also have been a few studies aimed at correlating the reactivity of young chars with their structural characteristics. Solid state <sup>13</sup>C and <sup>1</sup>H NMR have been adopted in the studies of various carbon and hydrogen functional groups of chars derived from short devolatilization times at temperatures up to 1250 K.<sup>17-19</sup> Their studies revealed, at the end of devolatilization, the carbon skeletal structures of chars from five coals of different rank are remarkable similar. This similarity in the carbon structure of the chars, however, is in marked contrast to the observed differences in their char reactivity. They have attributed these differences in char reactivity to second-order variations in the carbon skeletal structure that produce variations in active sites, surface area and pore structure and mineral contents.

Desorption of surface oxides is often considered the rate controlling step during char gasification with CO<sub>2</sub> and O<sub>2</sub>.<sup>20-24</sup> Several notable techniques involving chemisorption of CO<sub>2</sub> or O<sub>2</sub> of char and desorption of surface oxides have been developed, with the attempt to correlate the quantity and strength of surface oxides with char reactivity. Radovic et al.<sup>6,7</sup> concluded that deactivation of coal chars during gasification with increasing severity of pyrolysis conditions can be correlated with their active surface areas,<sup>25</sup> or ASA in short; ASA, in turn, is determined by oxygen chemisorption of chars at 375 K. Although some of their chars were prepared with short residence time, 0.3 s, at 700 to 1200°C, oxidation of chars were conducted in air at 550 to 750 K, a temperature range much lower than that in typical flames. Lizzio et al.<sup>21</sup> later

extended the ASA concept to the measurement of surface oxides of two different strengths, mobile and stable, through the experimental techniques of transient kinetics (TK) and temperature-programmed desorption (TPD). The surface area covered by mobile oxides was measured by TK; which showed better correlation with the char reactivity and is called reactive surface area (RSA).

At the outset of the current study, we seek to explore the correlations between the populations of surface oxides of different strengths on the chars and their origins and oxidation history. Experiments were focused on high temperature and short residence time conditions. Desorption techniques, including TK and TPD, are adopted in the characterization of young and old chars in situ in an alumina reactor.

As we will discuss in detail later, surprisingly large amounts of CO were observed in the TPD spectra of oxidized char between 1100 and 1700°C. Pan and Yang showed that stable oxides form on the basal planes of graphite and they desorbed completely during thermal treatment for 3 hours at 1500°C.<sup>26</sup> Nevertheless, the increasing trend of CO emissions at 1700°C during the TPD for coal-derived chars seem to suggest the occurrence of other reactions. To successfully accomplish our program goal, we have to determine the source and extent of these reactions in the interpretations of TPD products.

It is of our particular interest to find out the oxygen source of these CO emissions. Levy et al.<sup>27</sup> reported CO emissions at 1750 K from an alumina tube containing only coal-derived char. A CO “baseline” by feeding the char particles through the furnace under an inert atmosphere was measured; it was then subtracted from the CO yields in their study of (NO+CO) reaction. This procedure, however, generated difficulty in closing oxygen balance, and their conclusions on wall catalyzed (NO+CO) reaction and scavenging of surface oxides by CO are likely affected by their assumption of the oxygen source. To eliminate the possibility of oxygen emissions from the minerals in coal-derived chars and to reproduce the results of graphite by Pan and Yang<sup>26</sup>, we examined

the TPD products of graphite without prior oxidation. Interestingly, the CO yields quantitatively resemble those from coal-derived chars in the temperature range 1500 to 1700°C. Thus, the oxygen cannot come from the char.

The trace amounts of oxidants in He for TPD experiments were also suspected to be the source of oxygen. Nevertheless, TPD of graphite and pyrolyzed char in ultra high pure He further purified by copper turning 520°C and molecular sieve at liquid nitrogen temperature also demonstrated the same CO yields. Thus, the oxygen cannot come from the He.

Our attentions were then shifted to the roles of the reactor tubes of alumina and SiC and ceramic materials used in supporting the sample. Alumina tubes of 99.7% purity have been widely used in combustion laboratories. Indeed, some important conclusions have been drawn by using alumina tubes at temperatures above 1100°C in literature.<sup>27</sup> Thermodynamic properties<sup>28</sup> of Al<sub>2</sub>O<sub>3</sub> suggest it is stable and does not decompose in our temperature range, 1100 and 1700°C. Although the catalytic activity of alumina and other ceramic compounds on (CO + NO) reaction has been reported,<sup>27,12,29,25,30</sup> their potential chemical involvements in combustion systems have not been well known in or investigated by the fuel community.

This article presents our investigation on the existence of surface oxides on young chars derived from coals followed by our elucidation of the reactive involvements of commonly adopted ceramic tubes and supporting materials.

## **EXPERIMENTAL SECTION**

### **Experimental Apparatus**

As shown in Figure 1, a semi-flow alumina reactor equipped with a rapid coal-injection port has been designed, fabricated, and operated for the study of desorption of surface oxides. The U-shaped reactor is made of alsint of 99.7% of Al<sub>2</sub>O<sub>3</sub> from Bolt

Technical Ceramics with 1.27 cm I.D., 1.91 cm O.D., 500 mm in length, and 6.35 cm distance between the two centerlines of the two legs. The reactor was vertically placed in a Lindberg / Blue M Model 54494-V furnace equipped with 10 heating elements of 30.48 cm in length. The furnace has exterior dimensions of 55.88 cm in length, 40.64 cm in width, and 53.34 cm in height. The furnace temperature can be brought up to 1700°C by a programmable temperature controller, Lindberg / Blue M Model 59256-P-COM.

Oxidation and desorption products are analyzed by an online Agilent Technologies 6890 gas chromatograph and 5973N mass spectrometer (GC/MS). The base of the U-tube is typically positioned at the middle of the heating elements. The transport time between the reactor and the GC/MS is typically 14 or 22 s, depending on the gas flowrate.

The apparatus is designed so that char oxidation and desorption of surface oxides from char can be carried out *in-situ*. Desorption is usually conducted immediately after oxidation. Thus, contacts of char with foreign species are reduced to a minimal possible level.

In addition to the U-shaped alumina tube, a straight alumina tube and a straight SiC tube have been used to test the tube reactivity. These straight tubes were vertically placed inside the Lindberg / Blue M Model 54494-V furnace with a different set of insulation blocks at two ends.

Gas flows are controlled by specifically calibrated rotameters. A four-port sampling valve is installed before the reactor for switching gas, such oxidant and He, from one to another with minimal pressure and flowrate disturbance. The moisture in the product gas is removed by anhydrous calcium sulfate from W. A. Hammond Drierite Co. in a cartridge of 1.27 cm I.D. and 15.24 cm in length.

### **Particle Injection Methods**

For most tests reported here, the coal sample placed at the base of a stainless steel

tube of 0.952 cm I.D. concentric to the reactor tube was mechanically pushed into the preheated furnace by a piston. This method was later improved because the ceramic wool supporting the sample, which contained some coal particles, does not always be completely pushed to the base of the reactor where the temperature is highest.

Coal particles were later blown into the reactor by pressurized He stored in a 100 ml stainless steel gas-sampling cylinder vertically installed above the 0.952 cm I.D. tube described above. Coal particles, along with the supporting wool, were still kept at the base of the tube before injection. The cylinder is equipped with a pressure gauge and evacuation line to effectively purging the air out of the injection port by He. To quickly absorb the pressure surge caused by the injection, a 2-L stainless steel gas-sampling cylinder is installed in the downstream of the reactor. Before the injection, the up- and down-stream cylinders were kept at 7.8 atm and 0.164 atm, respectively. Upon the injection, the valves connecting with both cylinders are opened for about 2 s. The product gas is then switched back to the GC/MS line. The reactor pressure returns to the set pressure, 1.68 atm, within 2 s. The coal sample and the ceramic wool are effectively blown into the base of the reactor and stopped by ceramic wool, alumina beads and broken chips from used alumina tubes.

### **Transient Kinetics and Temperature-Programmed Desorption**

At the beginning of the transient kinetics (TK), about 1 gm of dried, pulverized coal is injected into the preheated reactor at 629°C or 1400°C with a He flow. After 2 min or 2 h pyrolysis time, the char is oxidized by switching the gas to a mixture of 20% O<sub>2</sub> balanced with He at 0.8 L/min for 15 s. Based on the rate constants of char oxidation report by Smith,<sup>3</sup> O<sub>2</sub> fed into the reactor is completely consumed and about 5% of carbon in the chars are burned out. Gas is then switched back to He, and the reactor is quenched naturally, at an initial rate about 36°C/min at 629°C. He flow is maintained at 0.8 L/min

and 80 ml/min for the production of chars with 2 min and 2 h pyrolysis times, respectively. Desorption products of weakly bound surface oxides during cooling reflects the transient kinetics (TK). The reactor pressure is maintained at 1.68 atm for all TK and TPD experiments.

Temperature-programmed desorption (TPD) is carried out as soon as the furnace temperature reaches 100°C after TK. TPD was initiated with 5°C/min heating rate up to 1700°C with a 75 ml/min He flow. The reactor is maintained at 1700°C for 90 min, and then it is cooled at 5°C/min rate.

Ultra-high-purity grade (NexAir) He with a minimum purity of 99.999% is used for TK and TPD. Oxidant impurities are guaranteed to be below 1 ppm. To minimize the presence of these oxidant impurities, they are removed by passing the gas through a alumina tube containing copper turnings maintained at 520°C by a Lindberg / Blue M Model TF55030A-1 furnace followed by a column of MS-13X molecular sieve (Duniway Stockroom Corp.) held at liquid nitrogen boiling temperature, a procedure established by Pan and Yang.<sup>31</sup>

In the study of reactions involving reactor wall and sample supporting materials, the same heating and cooling profiles as TPD are adopted. Nevertheless, the peak temperature and isothermal period at peak temperature might be different from run to run. Gas flowrate for these experiments is typically at 80 ml/min.

## **Samples**

A North Dakota Beulah lignite and an Illinois No.6 bituminous coal were ground; dried particles in the range of 100 to 140 meshes were used in oxidation and desorption experiments. Their ultimate and proximate analyses are shown Table 1. Synthetic graphite powder of -325 mesh from Alfa Aesar and of 99.9995% purity is also used in elucidating the reaction chemistry.

## **Reactor Tubes and Supporting Materials**

The U-shaped alumina tube is made of aluminite of 99.7% of  $\text{Al}_2\text{O}_3$  from Bolt Technical Ceramics (BTC). In addition to the U-shaped alumina tube, a straight alumina tube with 99.8% of  $\text{Al}_2\text{O}_3$  with 1.91 cm I.D., 2.54 cm O.D., 864 mm in length from McDanel Advanced Ceramic Technologies was also tested. The ceramic wool for supporting the coal sample before injection and blocking the coal inside the reactor is made of mulite, 72-75% of  $\text{Al}_2\text{O}_3$  and 25-28% of  $\text{SiO}_2$ , (or, PS-1500 fibermax – bulk) from the Unifrax Corporation. We also used alumina beads with the diameter of 0.32 to 0.47 cm and of the same composition as the tube from BTC to block the sample at the base of the reactor. The ceramic chips are broken pieces of the alumina tube.

It was later found that the SiC is more acceptable for TPD experiments in reducing environments. To design a new reacting system for the in-situ study of surface oxides, a straight SiC tube, SiC powders, a SiC foam and a SiC rod are tested for their interferences. The straight Hexoloy SA/SP SiC tube with 1.27 cm I.D., 2.54 cm O.D., 864 mm in length is acquired from Saint-Gobain Ceramics, see Table 2 for its composition. The SiC rod is made of the same material as the SiC tube. The SiC powders of two different sizes, F60 and F12 with a diameter of 212-300  $\mu\text{m}$  and 1400-2000  $\mu\text{m}$ , respectively, were acquired from the Industry Supply Co, Ltd., see in Table 3 for their compositions. The SiC foam is 0.635 cm thick, and has 60 pores per inch (PPI); it is acquired from the ERG and Aerospace Corp. It contains 66% Si and 34% C, and the impurities are shown in Table 4.

## **RESULTS AND DISCUSSION**

### **Transient Kinetics (TK) and Temperature-Programmed Desorption (TPD)**

Results from two coals, North Dakota lignite and Illinois No.6 coal, two ages, 2 s

and 2 h, and two oxidation temperatures, 629 and 1400°C are discussed in this section. The chars produced with 2 s and 2 h pyrolysis times are called young and old chars, respectively.

### ***Devolatilization, oxidation and TK at 629°C***

Figure 2 shows the CO and CO<sub>2</sub> yields during devolatilization and oxidation of 1 gm of coal at 629°C. The peaks at the extreme left are produced during pyrolysis, and the second set of peaks represent the products from oxidation. For the convenience of illustration, the oxidation peaks for the old chars were shifted closer their devolatilization peaks. Due to the production of volatiles, reactor pressure increases after coal is injected. A metering valve in the downstream is used to manually release the pressure; the system returns to its set pressure, 1.68 atm, within about 1 min. Thus, the product yields during the first min after injection is not considered quantitatively representative. As mentioned in the Experimental Section, the wool supporting the coal sample is sometimes trapped in the middle of the upstream leg of the reactor, and repeated push by the plunger is necessary to ensure the whole sample is pushed to the base of the reactor. The two small peaks associated with the old bituminous coal at about 5 min represent the CO and CO<sub>2</sub> yields from devolatilization after the second and third push; they are not from oxidation.

These four experiments were conducted with the same amount of O<sub>2</sub>, i.e., 20% of O<sub>2</sub> for 15 s. No O<sub>2</sub> was detected in their product streams. CO<sub>2</sub> is the principal product of char oxidation at 629°C. It is evident that young chars derived from both lignite and bituminous coal produce noticeably more CO<sub>2</sub> than their old chars during oxidation. Lignite chars produce more CO<sub>2</sub> than the chars derived from the bituminous coal. Young lignite char produces less CO than the young bituminous coal char.

The rate of decay of the CO peaks after gas switching under isothermal condition is typically called transient kinetics. We intend to preserve as much surface oxides as

possible for the TPD experiments, and the furnace power was shot off at the same time gas was switched. The decay of the CO<sub>2</sub> and CO peaks, however, still qualitatively represent the strength of the weakly bound surface oxides. The faster decay of oxides from young chars than those on the old chars suggests higher turnover rates of oxygen on young chars.

### ***Devolatilization, oxidation and TK at 1400°C***

Figure 3 shows the CO and CO<sub>2</sub> yields during devolatilization and oxidation of 1 gm of coal at 1400°C. CO is the main product of oxidation at 1400°C; very little CO<sub>2</sub> is produced from chars derived from the lignite and bituminous coal. Lignite chars, young and old, produce more CO than their counterparts derived from the bituminous coal. Young lignite char releases more CO than old lignite char, but the CO yields from young and old chars derived from the bituminous coal are comparable. This observation suggests that the crystalline structure of bituminous coal char stabilizes within 2 min of thermal treatment, an observation consistent with what Chen and Tang reported.<sup>12</sup> Surface oxides on young chars desorb faster than those on the old chars, and surface oxides on lignite chars desorb faster than those on the bituminous coal chars.

### ***Temperature-programmed desorption (TPD) at 629°C***

Figure 4 presents the TPD spectra of chars produced at 629°C. It is evident that young chars produce much more CO and CO<sub>2</sub>; lignite chars produce more desorption products than bituminous coal chars. CO productions are highest in three temperature ranges: 685-750°C, 1410-1455°C, and 1700°C. Chars from the bituminous coal seem to have another small peak at 1100°C. Notable CO<sub>2</sub> emission takes place only at about 700°C.

The TPD spectra in Figure 4 represent the rates of productions of CO and CO<sub>2</sub> at various temperatures under constant rate of heating. Assuming the desorption of surface oxides is a first-order reaction, the rate of production of a desorption product can be depicted by the equation derived by Juntgen and van Heek.<sup>32</sup>

$$\frac{dV}{dT} = \frac{K_0 V_0}{m} \exp \left[ -\frac{E}{RT} - \frac{K_0 R}{mE} T^2 \exp \left( -\frac{E}{RT} \right) \right]$$

where  $V$ ,  $T$ ,  $K_0$ ,  $V_0$ ,  $m$ ,  $E$  and  $R$  denote the production of volatile desorption product, temperature, frequency factor, overall yield of desorbed product, heating rate, activation energy, and ideal gas constant, respectively. Two of these parameters,  $K_0$  and  $E$ , are recovered from regressing experimental data in Mathcad.

Table 5 illustrates the parameter values from regression. The activation energies corresponding to CO desorptions from the chars at about 725°C vary from 100 to 170 kJ/mol, well within the range of those reported earlier.<sup>33</sup> Oxides on old chars have higher activation energies than those on young chars. Lignite chars have higher activation energies than chars derived from the bituminous coal. If we force the frequency factor to  $10^{10} \text{ min}^{-1}$  as suggested by collision theory,<sup>34</sup> the activation energies are consistently be to about 225 kJ/mol for all chars. It is not clear why the regressed frequency factors,  $10^4$  to  $10^7 \text{ min}^{-1}$ , are lower than those based on collision theory,  $10^{10} \text{ min}^{-1}$ . Nevertheless, it is interesting to note the extent of diffusion effects in the transfer line vary from lab to lab and it has not been fully investigated.

The abundant CO desorptions above 1100°C, especially those at 1700°C, as shown in Figure 4 have not the focus in a previous study or been reported for coal-derived chars. Nevertheless, the CO emissions at around 1430°C seem to suggest the existence of stable surface oxides on the coal-derived chars. Yang and coworkers<sup>31,37-39</sup> demonstrated that stable oxides form on the basal planes of the graphite, which

completely desorbed after heating in an inert gas at 1500°C for 3 h. XPS analysis and molecular orbital theory support their claims. Recently, Senneca et al.<sup>40</sup> presented HRTEM images illustrating the development of structural anisotropy during char oxidation, from which they postulate the possibility of formation of oxides on the basal planes of coal-derived chars. The rate constants,  $K_0$  and  $E$ , of the CO desorption peaks at around 1430°C are regressed, see Table 5. Oxides on the lignite chars have higher activation energies, about 430 kJ/mol, than those on the chars derived from the bituminous coal, 310 kJ/mol. Char's age does not seem to affect the activation energy. The frequency factor ranges from  $10^8$  to  $10^{12}$  min<sup>-1</sup> is closer to that based on the collision theory,  $10^{10}$  min<sup>-1</sup>. If we force  $K_0$  to be  $10^{10}$  min<sup>-1</sup>, the activation energies are consistently be to about 350 kJ/mol for all chars. It should be mentioned that the small CO-desorption peak at 1200°C for bituminous coal chars were subtracted from the main peak during the regression. The existence of these small peaks implies that the two activation-energies view, or the two-site view, may not be sufficient.

The existence of these stable surface oxides has several important implications and suggests the present knowledge of char combustion has to be better investigated. First, the rate-controlling step of char oxidation is likely to be governed by these stable oxides and thus have higher activation energies than what previously thought. Second, mechanistic conclusions are often drawn based on the assumption that all surface oxides desorb easily from the char surface above 900°C.<sup>41</sup> For instance, scavenging surface oxides by gaseous CO has not been thought to be an important reaction in flame conditions.<sup>27,30,42</sup>

### ***Temperature-programmed desorption (TPD) at 1400°C***

Figure 5 presents the TPD spectra of chars pyrolyzed and oxidized at 1400°C.

There are very small amounts of CO<sub>2</sub> productions at about 725°C. There are no notable CO emissions in the temperature range of 685-750°C implying the unstable nature of these weak surface oxides at 1400°C, as reflected by the large CO peaks during oxidation in Figure 3. Except for the young lignite char, the peaks at round around 1430°C are no longer obvious, likely due to the high oxidation temperature.

Again, there are large amounts of CO productions above 1100°C, which peak at the highest TPD temperature, 1700°C. These large CO productions puzzled us during the course of this study. Our first step was to conduct an oxygen balance. TPD spectra confirmed our calculations, based on the rate constants of char oxidation of Smith,<sup>3</sup> that all O<sub>2</sub> fed into the system during oxidation were completely consumed. Thus, the ratios of atomic oxygen as CO and CO<sub>2</sub> produced during oxidation and TPD to that in the feed O<sub>2</sub> represent recovered oxygen. Table 5 illustrates that this ratio is smaller than one when the oxidation peaks, TPD peaks at 725°C, and TPD peaks at 1430°C (shoulder area only) are included. However, the ratios were all greater than one when the major CO productions at 1700°C were considered suggesting the possibility of a major artifact in the experimental procedure. More importantly, the excessive CO productions during TPD at high temperatures became a serious obstacle for the study of surface oxides in flame conditions. To satisfactory resolve this problem, we developed a procedure for the elucidation of the chemical reactions involved in the systems, which will be discussed in the subsequent sections.

### **In Search of Oxygen Source for CO Production**

Since the alumina, especially alsint, have been widely adopted in combustion research, it has not been considered a possible source of oxygen production.<sup>27</sup> Indeed, according to the Ellingham Diagram,<sup>43</sup> the equilibrium parameter of the reaction

$2Al_2O_3 \rightarrow 4Al + 3O_2$  is very low, where the oxygen partial pressure is only  $2.84 \times 10^{-20}$  atm at 1900 K. Thus, our initial search for the oxygen source was placed on coal, chars and impurities in the gas.

To investigate if the excess CO production is really the desorption product of surface oxides formed during oxidation, a pyrolysis run with the Illinois #6 coal was conducted followed by in-situ TPD. The aforementioned experimental procedure for oxidized chars was adopted, but no oxidation was introduced into the system. The resultant TPD spectrum showed CO yield of the same magnitude as those presented in Figure 5 at high temperatures. Thus, the excessive CO cannot be the decomposition products of surface oxides. Nevertheless, the effects of char's minerals cannot be completely excluded.

It was also suspected that the CO production might be due to the volatiles and tars condensed on the ceramic wool and tube wall in the downstream of the tube during pyrolysis. To exclude the effects of this source, a char was prepared from a separated pyrolysis unit described by Chen and Tang,<sup>12</sup> where 12 gm of Illinois No.6 coal sample was pyrolyzed in an alumina basket in a preheated alumina tube at 1100°C for 2 h. TPD was then conducted with 1 gm of this char placed at the bottom of the U-shape tube. Once again, the same amount of CO yield as those shown in Figure 5 was observed at high temperatures, suggesting that volatiles condensation from coal pyrolysis are not a source of CO production in TPD.

It was suspected that adsorption of trace amounts of oxidative impurities in the ultra high pure He on char at low temperature might cause formation of undesirable surface oxides and eventually lead to CO production. To remove such impurities, He was passed through by a copper-turning bed maintained at 520°C followed by a column of MS-13X molecular sieve immersed in liquid N<sub>2</sub> at 77 K before it entered the reactor.<sup>[26]</sup>

This purification treatment is effective in removing all oxidants in He detectable by MS, and is used in all subsequent experiments. Nevertheless, TPD of pyrolyzed char still demonstrated the same CO yields, thus, the impurities in the He is not source for CO production.

It was observed that, after several TK/TPD experiments, the inside wall of the U-shape tube near the coal sample became dark. It does not appear to be coal derived liquids or minerals because it does not dissolve in either strong organic solvent, such as 1,2,3,4-tetrahydroquinoline, or 3M nitric acid over night. Thus, the role of char's minerals, such carbonates, became a point of interest in the search of oxygen source. A TPD experiment was then conducted with a graphite sample placed at the base of the U-tube. Graphite is chosen because it is essentially mineral free. Trace I in Figure 6 illustrates that the CO production from the (graphite + tube) experiment is about the same magnitude as coal-derived chars shown in Figures 4 and 5 at 1700°C. Therefore, minerals in chars are not responsible for the CO production. In fact, contrary to what Levy et al.<sup>27</sup> claimed, char as a whole is not a source. It should also be pointed out that the absence of CO peak at 1430°C in trace I of Figure 6 further supports the conclusion that those CO peaks in Figure 4 represent stable surface oxides.

In conclusion, the excessive CO productions at 1700°C do not represent surface oxides formed during oxidation. Minerals in chars and He gas are not the source either. Our focus at this moment is shifted to the roles of reactor tube and its support materials.

## **Roles of Reactor Materials**

### ***Alumina tube***

Our first test in the elucidation of the wall involvements was a run with an empty alumina U-tube heated up to 1650°C with a 5°C/min ramp identical to a TPD experiment.

A new U-shaped tube was used in this test. As illustrated by the trace III in Figure 6, the tube starts to emit detectable O<sub>2</sub> at about 1400°C and the emission increases to about 112 ppm at 1600°C. These results were not expected since the observed O<sub>2</sub> concentrations are much higher than those estimated under equilibrium. According to the Ellingham Diagram<sup>43</sup> and the thermodynamic property data of the JANAF Thermochemical Tables,<sup>28</sup> the O<sub>2</sub> partial pressures at equilibrium when Al<sub>2</sub>O<sub>3</sub> decompose to form Al and O<sub>2</sub>, or,  $2Al_2O_3 \rightleftharpoons 4Al + 3O_2$ , are only about  $4.64 \times 10^{-26}$  and  $2.84 \times 10^{-20}$  atm at 1600 and 1900 K, respectively. Al<sub>2</sub>O<sub>3</sub> also decomposes to a few sub-oxides; among them  $Al_2O_3 \rightleftharpoons Al_2O_{(g)} + O_2$  is the most important route at high temperatures. Based on the data of JANAF Tables, however, the O<sub>2</sub> partial pressures at equilibrium are only about  $1.70 \times 10^{-15}$  and  $1.19 \times 10^{-11}$  atm at 1600 and 1900 K, respectively.

To remove the possible residue carbon retained on the reactor wall after TPD, we routinely burn the empty alumina tube at 1650°C with 20% O<sub>2</sub> in He. This procedure was suspected to be source of oxygen emissions in later experiments. Nevertheless, a fresh new tube also emits the same amount of O<sub>2</sub>, therefore, the oxidation procedure after TPD cannot be the source of oxygen.

Although it is not clear why we observe high O<sub>2</sub> concentrations, it is known that Al<sub>2</sub>O<sub>3</sub> reacts with reducing agents, such as carbon and CO, and yields Al<sub>2</sub>O<sub>(g)</sub>. Cochran<sup>44</sup> noted that the (Al<sub>2</sub>O<sub>3</sub> + C) system forms an ideal liquid solution of Al<sub>2</sub>O<sub>3</sub>, Al<sub>4</sub>C<sub>3</sub>, and Al<sub>4</sub>O<sub>4</sub>C above 2200 K and 1 atm. When the temperature was further increased, it forms ideal liquid solution of Al, C, and Al<sub>4</sub>C<sub>3</sub>. Yokokawa et al.<sup>45</sup> and Wai and Hutchison<sup>46</sup> investigated the carbothermic reduction of alumina and reported the product distributions, including CO<sub>(g)</sub>, and stability diagram of the Al-O-C system based on JANAF tables; the latter includes stability boundaries of elemental aluminum relative

to its carbides, oxides, and other species at various temperatures. It is possible that the dark materials that form on the inner wall of the tube and packing materials are the condensed volatile mixture of aluminum oxycarbide alloys.

Based on the data of JANAF Thermochemical Tables, the CO partial pressures at equilibrium when alumina undergoes carbothermic reduction, or,

$Al_2O_3 + 2C \rightleftharpoons Al_2O + 2CO$ , are  $4.40 \times 10^{-5}$  and  $6.38 \times 10^{-3}$  atm at 1600 and 1900 K,

respectively. These concentrations are in good accordance with our experimentally observed CO yields. As illustrated in Figure 4, the CO yields from the (char +  $Al_2O_3$ ) system are about 7000 ppm. Trace I in Figure 6 shows that the CO yield from the (graphite +  $Al_2O_3$ ) system is about 6000 ppm.

To evaluate the impact of oxygen emissions on the analysis of CO during TPD and to better understand the tube chemistry, a gas mixture containing 0.8 vol% of CO balanced with He was passed through the alumina reactor tube that was heated with a heating ramp 5°C/min. Trace II in Figure 6 represents the CO<sub>2</sub> yields from this experiment. It appears that CO reacts with  $Al_2O_3$  and forms CO<sub>2</sub>, i.e.,

$Al_2O_3 + 2CO \rightleftharpoons Al_2O + 2CO_2$ . Nevertheless, while the observed CO<sub>2</sub> production is about 700 ppm at 1650°C, the calculated yield based on JANAF Tables is only about 20 ppm at 1650°C. Similar to the O<sub>2</sub> emissions, the actual production of oxygen is higher than those predicted suggesting the participations of other reactions. Impurities in the tube may consist a source of additional oxygen.

The CO concentrations decline in the isothermal regions in Figures 4 through 6. It is known that exposure of mass spectrometer detector to species at high concentrations over a long period of time can cause relaxations. Alternatively, the mass transfer resistance due to the formation of an aluminum oxycarbide layer may cause the decreases. To distinguish these causes, a gas mixture containing only 325 ppm of CO

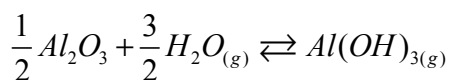
was passed through the alumina reactor tube that was heated with a heating ramp  $5^{\circ}\text{C}/\text{min}$ . As expected, the exit CO concentration between 500 and  $1000^{\circ}\text{C}$  remains steady. The stoichiometrically consistent  $\text{CO}_2$  increase and CO increase over a wide temperature range supports the postulated reaction above. It is interesting to note that CO and  $\text{CO}_2$  concentrations continue to decrease and increase, respectively, during the isothermal period  $1650^{\circ}\text{C}$ . Thus, the declines observed in the isothermal periods in Figures 4 through 6 are likely caused by the relaxation of the MS detector. The increase in  $\text{CO}_2$  observed in Figure 7 may be contributed by a different physical mechanism at low feed CO concentration. Intuitively, CO at low concentrations can cause gradual increase in pore surface areas, therefore, enhancement in rate of reaction of CO with the alumina tube. At high CO concentrations, reaction takes places layer by layer like the shrinking core model, and the rate of reaction remains the same.

It is known that surface-to-volume ratio and gas residence time affect wall reactions. An experiment was conducted to provide additional evidences of wall effects. The U-shaped tube with 500mg of graphite in the bottom was heated to  $1200^{\circ}\text{C}$  with a heating rate  $5^{\circ}\text{C}/\text{min}$  and a He flow rate 100 cc/min. The flow rate was changed to 250 ml/min and 500 ml/min at the peak temperature. Figure 8 illustrates that the CO concentration decreases as the flow rate increased. The dependence of flow rate implies kinetically controlled wall reactions. Pan and Yang reported that CO concentration from oxidized graphite during TPD decreases to zero when the reactor is maintained at  $1500^{\circ}\text{C}$  for several hours suggesting the importance of operating variables.

The extent of CO reaction with the tube may not be a serious issue as we observe no or very low yields of  $\text{CO}_2$  at high temperatures during TPD, see Figures 4 and 5. Nevertheless, oxygen emission from the alumina tube and reaction of alumina with carbon above  $1200^{\circ}\text{C}$  distort the true speciation of TPD products. These problems are

detrimental to the study of stable surface oxides on coal-derived chars, a subject that has not been a focus of previous studies yet alumina tubes have been the most commonly used in combustion laboratories. Alternative tube materials and experimental means have to be developed for the study of study of stable oxides at high temperatures. Silicon carbide tubes have also been used in combustion laboratories, thus, a SiC tube was then selected for the next set of tests.

We did not investigate the reaction of alumina with water vapor, another commonly encountered oxidant in combustion process. It should be mentioned that Opila and Myers<sup>47</sup> found that alumina reacts with water vapor and form volatile hydroxide in the temperature range 1250 to 1500°C. The reaction can be presented as follows:



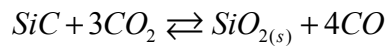
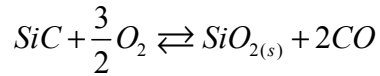
### ***Silicon carbide (SiC) tube***

A straight Hexoloy SA/SP SiC tube was heated to 1650°C with a heating rate 5°C/min and with the following flowing gases or gas mixtures: highly purified He, and O<sub>2</sub>, CO and CO<sub>2</sub> in He. During the runs with highly purified He, we observed no notable emissions of O<sub>2</sub>, CO or CO<sub>2</sub>.

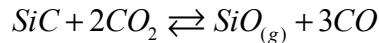
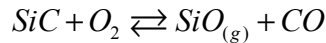
Figure 9 illustrates the speciation from heating the SiC tube with flowing 300 ppm O<sub>2</sub> in He at an overall flow rate of 80 ml/min. Productions of CO and CO<sub>2</sub> above 650°C suggest the oxidation of SiC. CO<sub>2</sub> forms only between 700 and 1250°C. To understand the extent of SiC oxidation, feed O<sub>2</sub> concentration was gradually increased at 1600°C in a separated experiment, excess O<sub>2</sub> started to appear in the product stream after its feed concentration was increased to slightly below 4 vol% (not shown in Figure 9). Higher concentrations of O<sub>2</sub> shift the reaction product to higher concentrations of CO<sub>2</sub>.

Figure 10 illustrates the speciation from heating the SiC tube with flowing 100 ppm CO<sub>2</sub> in He at an overall flow rate of 80 ml/min. Oxidation begins at about 900°C and CO<sub>2</sub> is converted to CO. It reaches an unexpectedly high concentration of CO at 1600°C, and oxygen balance cannot be closed. This extra amount of CO is likely due to the reduction of the scale of SiO<sub>2(s)</sub> formed on the inner wall of the tube during the present and previous oxidation experiments. These mechanisms are discussed in detail below.

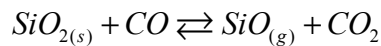
SiC is thermally unstable. In highly oxidizing environments, a layer of SiO<sub>2(s)</sub> scale forms on the SiC, which is called “passive oxidation.”<sup>48</sup>



In weak oxidants or low oxidant partial pressure, SiC is oxidized to SiO<sub>(g)</sub>, no SiO<sub>2(s)</sub> layer forms. This mechanism is called “active oxidation.”<sup>48</sup>



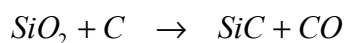
Active oxidation may also take place in the presence of other agents, such as mixtures containing CO. In this case, the oxidation product SiO<sub>2(s)</sub> is converted to SiO<sub>(g)</sub> by CO. Opila and Jacobson demonstrated that SiO<sub>(g)</sub> forms in mixtures of oxidizing-reducing gases<sup>49</sup>:



In our experiments with 300 ppm O<sub>2</sub> and 2500 ppm CO<sub>2</sub> presented in Figures 9 and 10, oxidants are completely consumed above 1250°C. Therefore, though formation of SiO<sub>2(s)</sub> layers is expected below 1250°C, transition of passive to active oxidation is likely when temperature increases. These observations are consistent with those reported by

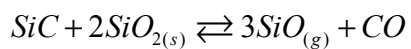
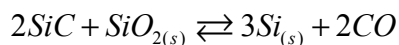
Gulbransen and Jansson<sup>48</sup> and Opila and Jacobson.<sup>49</sup>  $\text{SiO}_{(g)}$  condenses before it reaches GC/MS and we did not attempt to analyze it. However,  $\text{CO}_2$  is found between 700 and 1250°C when SiC is oxidized by  $\text{O}_2$ , see Figure 9, suggesting the passive oxidation of CO by both  $\text{O}_2$  and  $\text{SiO}_{2(s)}$ . Moreover, as the feed  $\text{O}_2$  concentration was gradually increased until  $\text{O}_2$  becomes excess at 1600°C, passive oxidation takes over and a layer of  $\text{SiO}_{2(s)}$  was indeed observed in the hot zone of SiC tube.

Once  $\text{SiO}_{2(s)}$  forms on the tube wall, it reacts with char, produces CO and distorts TPD results through the reaction below



Therefore, contacts SiC with oxidants should be avoided to ensure the data integrity from TPD experiments.

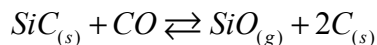
Gulbransen and Jansson reported the complexity of the Si-O-C system and the transition from passive to active oxidation.<sup>48</sup> They noted high ( $\text{SiO}_{(g)} + \text{CO}$ ) and  $\text{SiO}_{(g)}$  pressures at the  $\text{SiC}_{(s)} - \text{SiO}_{2(s)}$  and  $\text{Si}_{(s)} - \text{SiO}_{2(s)}$  interfaces, respectively, which, in turn, are governed by the following three reactions:



Interestingly, the thermal reactions mentioned above can be used to restore the SiC surface for TPD experiments. Figure 11 demonstrated that CO emission from an oxidized SiC tube reduces to zero when the tube is heated with flowing He at 1650°C for about 4 h. Nevertheless, the phase diagrams reported by Gulbransen and Jansson suggest that formation of  $\text{Si}_{(s)}$  and  $\text{C}_{(s)}$  are possible, and oxidation of SiC tube should be avoided before TPD experiments.

In our study of the reaction of SiC with 3000 ppm CO in He, only a small amount

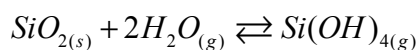
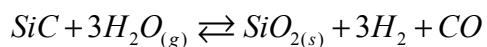
of 65 ppm CO<sub>2</sub> was observed in the temperature range 1220 to 1630 K, and other species, including CO, remain constant. According to Gulbransen and Jansson,<sup>48</sup> CO oxidizes SiC and the SiC surface becomes blackened above 1573 K and at 1 atm CO. At 1800 K, the main reaction is:



Based on their phase diagram, the partial pressure of SiO<sub>(g)</sub> is only 5.534 · 10<sup>-6</sup> atm when CO is at 1000 ppm. In our TPD experiment CO production is no more than several thousand ppm, and, therefore, the extent of CO loss due to this reaction is not likely to be significant. Gulbransen and Jansson also predicted the formation of a small amount of CO<sub>2</sub> from (SiC+CO) reaction below 1600 K, which is consistent with what we observed. This CO<sub>2</sub> production is not expected to cause highly detrimental effects on the analysis of surface oxides from chars.

Based on our observations and published works, SiC tube appears to be a good candidate for experiments in reducing environments, such as TPD, at temperatures between 1100 and 1700°C. The products, Si<sub>(s)</sub> and C<sub>(s)</sub>, are not expected to affect our TPD result significantly, other than consuming a small part of desorbed CO from the oxidized char.

We did not investigate the reaction of SiC with water vapor. It should be mentioned, however, that CO forms in this reaction and may distort the desirable data. Specifically, Opila<sup>50</sup> and Robinson and Smialek<sup>51,52</sup> reported the following sequential reactions in the temperature range 1200 to 1400°C:



Therefore the water trapped in the tube after cleaning and the moisture in the feed gas has to be removed before it enters the reactor. In order to remove the moisture attached to the

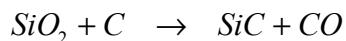
tube after cleaning with water, the SiC tube was heated at 200°C in vacuum for 3 hours.

### ***Supporting materials in tubes***

In our experiments with the U-shaped alumina tube, ceramic wool, ceramic beads and chips were used to support the sample before or after coal injection. In the SiC-tube experiments, SiC foam, SiC powder and SiC rod were used. Their potential interferences on the study of surface oxides on chars are assessed below. Since the beads and chips are made of the same materials as the alumina tube, we decided not to adopt them as soon as we observed the oxygen emission problem.

Ceramic wool is an indispensable material for our experiments because it is one of the few soft materials that can be used to support the particles and sustain temperatures up to 1700°C. Nevertheless, ceramic wool contains 72-75% of Al<sub>2</sub>O<sub>3</sub> and 25-28% of SiO<sub>2</sub>, its high content of SiO<sub>2</sub> render it much susceptible to O<sub>2</sub> release than Al<sub>2</sub>O<sub>3</sub>. A thermal test was conducted to verify our concern. A sample of about 0.65 gm of ceramic wool was placed in the middle of a SiC tube and supported by a SiC foam and a SiC rod. The tube was heated to 1650°C at 5°C /min with a flow of 80 ml/min He. Figure 12 illustrates that a significant amount of CO is released at high temperatures, with a trend similar to the experiment with a blank alumina tube shown in Figure 6. Moreover, a small amount of CO<sub>2</sub> also detected at lower temperatures; its source is not clear. Brown deposits were observed on the surface of the rod in the cold section where the volatile minerals started to cool.

In addition to CO and CO<sub>2</sub> emissions, as mentioned earlier, SiO<sub>2</sub> reacts with char and releases CO during TPD



Calculations based on total Gibbs' free energy change suggest this carbothermal

reduction becomes significant at temperature above 1200°C. This reaction is known in manufacturing of biomorphic SiC ceramics by sol-gel processing, see Brinker and Scherer<sup>53</sup> and Rambo et al.<sup>54</sup> Thus, the ceramic wool may be acceptable in oxidizing environments that allows small amount of O<sub>2</sub> and CO<sub>2</sub> emissions, it is not acceptable for TPD.

Sample supporting materials, SiC foam, rod and powders, were then tested in TPD environment. The rod supports the foam and 10 gm beads of 2 different sizes in the middle of the SiC tube. The circular foam is cut from the sheet with an 80-degree angle so that the cross-section of the foam appears as a trapezoid. The diameter of circular foam at its base is about the same as the ID of the tube, so that the foam can be pushed in easily. Small space between the tube and the foam is filled with a small amount of the smaller beads, F60. Larger beads, F12, were placed on the top of the foam, and another layer of smaller beads, F60, is placed above the larger beads. This arrangement is to avoid direct contact of char particles with the porous foam so we can reuse the expensive foam, and the pressure drop across the bed is nominal. The tube was then heated two consecutive times to 1650°C with flowing He. Figure 13 illustrates an 1000 ppm CO emission at 1650°C and 30 ppm CO<sub>2</sub> emission at 500°C, respectively, during the first heating. These emissions significantly decrease during the second heating. Since the rod and foam have been used in previous TPD experiments with chars and wool, the CO emission during heat treatment is likely the product of the reaction of SiC with SiO<sub>2(s)</sub> scale. It may also be caused by impurities in the beads. CO<sub>2</sub> production is not clear. Heat treatment seems to be an effective way of suppressing CO and CO<sub>2</sub> emissions and restoring oxidized SiC materials for TPD experiments.

## **Suggestions on the Reactor Configuration for *In-Situ* Study of Surface Oxides**

Our findings discussed above suggest the alumina and SiC tubes can be used to for oxidation and TPD environments, respectively. A two-stage reacting system involving these two different types of reactor tubes appears acceptable for the study of reactivity of young chars in-situ. The results from a two-stage system will be reported in subsequent papers.

## **CONCLUSIONS**

Young chars retain more abundant surface oxides than those on old chars over a wide range of temperatures. Oxygen-turnover rates on young chars are much higher than those on old chars. Chars derived from lignite possess larger amounts of surface oxides than those on the chars derived from a bituminous coal. Chars oxidized at 629°C release CO during TPD at about three distinct temperatures: 725, 1430 and 1700°C. The CO desorption peak at 725°C has been well reported in the literature, while the two others are not. The oxides desorbed at around 1430°C have activation energies over 300 kJ/mol, suggesting the presence of relatively stable oxides on the basal plan of the carbon. These oxides are not completely stable in flame since chars oxidized at 1400°C do not show very clear peaks at 1430°C during TPD. Nevertheless, desorption of these stable oxides may be the rate-controlling step during char combustion.

In the study of the huge CO productions at 1700°C during TPD, our focus was shifted to wall-participated reactions. It was discovered that alumina tube and sample support materials emits O<sub>2</sub> above 1300°C. They react with CO and forms CO<sub>2</sub>; they also react with carbon and form CO and aluminum oxycarbides. These reactions distort the TPD data and render alumina unfit for the TPD experiments at high temperatures. SiC tube and sample support materials were examined as possible replacements. Although they react with oxidants, including O<sub>2</sub>, CO<sub>2</sub> and H<sub>2</sub>O, they emit no oxidants and react

with CO at a very low level. They appear suitable for TPD above 1200°C. Oxidized SiC tube can be restored for TPD simply by heat treatment at 1650°C, though accidental oxidation should be avoided.

## ACKNOWLEDGMENT

The authors wish to acknowledge the financial support of the National Science Foundation under grant CTS-0122504. Dr. Elizabeth J. Opila and Dr. Alejandro Molina provided valuable information during the course of this study. The authors would also like to thank George Gowan, Thomas Taylor, Samuel Ridge, Kimberly Thames, Emily Faulks and Mark Shows for their technical supports.

## REFERENCES

1. Smoot, L.D; Smith, P.J. *Coal combustion and gasification*. New York: Plenum Press, 1985.
2. Howard, J.B. *Elliott MA, John Wiley ED. Chemistry of coal utilization, second supplementary volume*, New York 1981, 665-784.
3. Smith, I.W. *The Combustion Institute, 19th Symp. (Int'l) on combustion. Pittsburgh, PA 1982*, 1045-1065.
4. Teng, H; Suuberg, E.M; Calo, J.M. *Energy & Fuels* **1992**, 6, 398-406.
5. Suuberg, E.M. *Lahaye ed J, Ehrburger P. Fundamental issues in control of carbon gasification reactivity*. The Netherlands: Dordrecht, Kluwer Academic Publishers, 1991, 269-305.
6. Radovic, L.R; Walker, J.P.L; Jenkins, R.G. *J. of Catalysis* **1983**, 82, 382-394 .

7. Radovic, L.R; Walker, J.P.L; Jenkins, R.G. *Fuel* **1983**, *62*, 849-856.
8. Hurt, R.H.; Davis, K.A.; Yang, N.Y.C.; Headley, T.J.; Mitchell, G.D. *Fuel* **1995**, *74*, 1297-1306.
9. Sahu, R; Levendis, Y.A; Flagan, R.C; Gavalas, G.R. *Fuel* **1988**, *67*, 275-283.
10. Wong, B.A; Gavalas, G.R; Flagan, R.C. *Energy & Fuels* **1995**, *9*, 493-499.
11. Nagle, J; Strickland-Constable, R.F. *Proc. 5th Conf. on Carbon, Pergamon Press* **1962**, *1*, 154-164.
12. Chen, W.Y; Tang, L. *AIChE Journal* **2001**, *47*, 2781-2797
13. Chen, W.Y.; Gathitu, B. B. *Fuel* **2006**, *85*, 1781-1793.
14. Dictor, A.D. *Determination of Complete Temperature Profiles of Singly Burning Pulverized Fuel Particles*, Master thesis, M.I.T, Dept. of Chemical Engineering, Cambridge, Mass., 1979.
15. Molina, A; Eddings, E.C; Pershing, D.W; Sarofim, A.F. *Proceedings of the combustion institute* **2002**, *29*, 2275-2281.
16. Garijo, E.G; Jenson, A.D; Glarborg, P. *Combustion and Flame* **2004**, *136*, 249-253.
17. Fletcher, T.H; Solum, M.S; Grant, D.M; Critchfield, S; Pugmire, R.J. *23<sup>rd</sup> (Int'l) Symposium combustion. Pittsburgh, PA: The Combustion Institute* **1991**, 1231-1237.
18. Pugmire, R.J; Solum, M.S; Grant, D.M; Critchfield, S; Fletcher, T.H. *Fuel* **1991**, *70*, 414-423.

19. Fletcher, T.H; Solum, M.S; Grant, D.M; Pugmire, R.J. *Energy and Fuels* **1992**, 2, 18-26.
20. De Soete, G.G. *Pulverized coal combustion: pollutant formation and control, 1970-1980. EPA-600/8-90-049*, **1990**, 8,1-59.
21. Lizzio, A.A. *The concept of reactive surface area applied to uncatalyzed and catalyzed carbon (char) gasification in carbon dioxide and oxygen*. PhD Dissertation, Department of Material Science and Engineering, The Pennsylvania State University, **1990**.
22. Teng, H; Suuberg, E.M; Calo, J.M. *Energy & fuel* **1992**, 6, 398-406.
23. Illan-Gomez, M.J; Linares-Solano, A; Radovic, L.R; Salinas-Martinez de Lecea, C. *Energy & fuels* **1996**, 10, 158-168.
24. Illan-Gomez, M.J; Salinas-Martinez de lecea, C; Linares-Solano, A; Phillips, J; Radovic; L.R. *Preprints of the div. of fuel chem., Am. Chem. Soc.* **1996**; 41, 174-178.
25. Laine, N.R; Vastola, F.J; Walker, J.P.L. *J. Phys. Chem.* **1963**, 67, 2030-2034.
26. Pan, Z.; Yang, R.T. *Ind Eng Chem Res* **1992**, 31, 2675-2680.
27. Levy, J.M; Chan, L.K.; Sarofim, A.F.; Beer, J.M. *Eighteenth Symposium (Int'l) on Combustion, the Combustion Institute* **1981**, 111-120.
28. Chase, M.W.Jr.; Davies, C.A.; Downey, J.R.Jr.; Frurip, D.J.; McDonald, R.A.; Syverud, A.N. *JANAF Thermochemical Tables, Third Edition*, American Institute of Physics, Inc., New York, 1985.
29. Wittler, W.; Schutte, K.; Rotzoll, G.; Schugerl, K. *Fuel* **1988**, 67, 438-440.

30. Aarna, I.; Suuberg, M.E. *Energy and Fuels* **1999**, *13*, 1145-1153.
31. Pan, Z.; Yang, R.T. *Ind Eng Chem Res* **1992**, *31*, 2675-2680.
32. Juntgen, H.; Van, K.H. *Fuel* **1968**, *47*, 103-117.
33. Calo, J.M.; Hall, P.J. *Fundamental Issues in Control of Carbon Gasfication Reactivity*, Kluwer Academic Publishers, Dordrecht/Boston/London, 1991, 329-368.
34. Masel, R.I. *Chemical Kinetics and Catalysis*, John Wiley & Sons, Inc., 2001.
35. Redhead, P.A. *Vacuum* **1962**, *12*, 203-211.
36. Du, Z.; Sarofim, A.F.; Longwell, J.P. *Energy & Fuels* **1990**, *4*, 296-302.
37. Duan, R.Z.; Yang, R.T. *Chemical Engineering Science* **1984**, *39*, 795-798.
38. Yang, T.R.; Wong, C. *J. Chem. Phys.* **1981**, *75*, 4471-4476
39. Chen, N.; Yang, T.R.; Goldman, S.R. *Journal of Catalysis* **1998**, *180*, 245-257
40. Senneca, O.; Salatino, P.; Masi, S. *Proc. Combust. Inst.* **2005**, *30*, 2223-2230.
41. Teng, H.; Suuberg, M.E.; Calo, M.J. *Energy & Fuels* **1992**, *6*, 398-406.
42. Molina, A.; Eddings, E.G.; Pershing, D.W.; Sarofim, A.F. *Combustion and Flame* **2004**, *136*, 303-312.
43. Gaskell, D.R. *Introduction to Metallurgical Thermodynamics, Second Edition*, Hemisphere Publishing Corporation, Washington, 1981.
44. Cochran, N.C. *Metal-Slag-Gas Reactions and Processes*, The Electrochemical Society, Inc., Princeton, NJ, 1975, 299-316.

45. Yokokawa, H.; Fujishige, M.; Ujiie, S.; Dokiya, M. *Metallurgical Transactions B* **1987**, *18B*, 433-444.
46. Wai, M.C; Hutchison, G.S. *Metallurgical Transactions B* **1990**, *21B*, 406-408
47. Opila, J.E.; Myers, L.D. *Journal of the American Ceramic Society* **2004**, *87*, 1701-1705.
48. Gulbransen, A.E; Jansson, A.S *Oxidation of Metals* **1972**, *4*, 181-201
49. Opila, J.E.; Jacobson, N.S. *Oxidation of Metals* **1995**, *44*, 527-544
50. Opila, J.E. *Journal of the American Ceramic Society* **2003**, *86*, 1238-1248.
51. Opila, J.E.; Smialek, L.J.; Robinson, C.R.; Fox, S.D.; Jacobson, S.N. *Journal of the American Ceramic Society* **1999**, *82*, 1826-1834.
52. Robinson, C.R.; Smialek, L.J. *Journal of the American Ceramic Society* **1999**, *82*, 1817-1825.
53. Brinker, C.J.; Scherer G.W. *Sol-Gel Science*, Academic Press, Inc., San Diego, 1990.
54. Rambo, R.C.; Cao, J.; Rusina, O.; Sieber, H. *Carbon* **2005**, *43*, 1174-1183.

**Table 1. Ultimate and Proximate Analyses of Coals (dry basis)**

| Content, %        | North Dakota Beulah lignite | Illinois No.6 Bituminous |
|-------------------|-----------------------------|--------------------------|
| Carbon            | 65.14                       | 72.9                     |
| Hydrogen          | 4.33                        | 4.9                      |
| Oxygen            | 18.44                       | 6.6                      |
| Nitrogen          | 0.97                        | 1.5                      |
| Sulfur            | 1.24                        | 2.8                      |
| Volatile material | 42.76                       | 35.8                     |
| Fixed carbon      | 47.73                       | 53.3                     |
| Ash               | 9.8                         | 10.8                     |

**Table 2. Composition of Hexoloy silicon carbide**

|         |         |         |         |         |       |         |       |
|---------|---------|---------|---------|---------|-------|---------|-------|
| SiC     |         | Al      | B       | C       | Ca    | Cr      | Cu    |
| 98(wt%) |         | 132ppm  | 6900ppm | 5300ppm | 7ppm  | <0.3ppm | <1ppm |
| Fe      | K       | Na      | Ni      | Ti      | V     | Zn      | Zr    |
| 6ppm    | <1.3ppm | <0.6ppm | <3ppm   | 18ppm   | 17ppm | 1ppm    | 5ppm  |

**Table 3. SiC powder composition mass %**

|          |           |            |                    |
|----------|-----------|------------|--------------------|
| SiC      | Fe (Iron) | C (carbon) | Magnetic admixture |
| Min. 98% | Max 0.3%  | Max 0.3%   | Max 0.2%           |

**Table 4. Impurities in SiC foam, ppm**

|        |       |       |       |        |        |       |       |       |       |        |         |
|--------|-------|-------|-------|--------|--------|-------|-------|-------|-------|--------|---------|
| B      | Na    | Al    | P     | S      | K      | Ti    | V     | Cr    | Mn    | Fe     | Bi      |
| 0.7    | 0.12  | 0.086 | 0.022 | 13     | <0.057 | 0.034 | 0.018 | <0.35 | 0.025 | <0.10  | <0.0049 |
| Co     | Ni    | Cu    | Zn    | Ga     | Zr     | Mo    | Ag    | Sn    | Ba    | W      | Pb      |
| 0.0068 | 0.045 | 0.12  | 7.6   | <0.026 | <0.010 | 0.13  | 0.071 | 0.45  | 0.047 | <0.011 | <0.0067 |

**Table 5. Surface oxide and activation energy**

|                         |                 | Surface Oxide, ml/gm coal |              |             | Oxygen Balance <sup>(a)</sup> | Rate Constants <sup>(b)</sup> |                       | Rate Constants <sup>(c)</sup> |                       |
|-------------------------|-----------------|---------------------------|--------------|-------------|-------------------------------|-------------------------------|-----------------------|-------------------------------|-----------------------|
|                         |                 | TK, 629°C                 | TPD, <1100°C | TPD, 1430°C |                               | Fraction                      | K0, Min <sup>-1</sup> | E, kJ/mol                     | K0, Min <sup>-1</sup> |
| <b>Young Lignite</b>    | CO              | 1.33                      | 14.36        | 4.00        | 0.37                          | 2.57*10 <sup>5</sup>          | 130                   | 7.95*10 <sup>12</sup>         | 443                   |
|                         | CO <sub>2</sub> | 3.91                      | 0.91         |             |                               |                               |                       |                               |                       |
| <b>Old Lignite</b>      | CO              | 1.05                      | 10.03        | 3.68        | 0.29                          | 1.2*10 <sup>7</sup>           | 170                   | 1.40*10 <sup>12</sup>         | 423                   |
|                         | CO <sub>2</sub> | 3.52                      | 0.56         |             |                               |                               |                       |                               |                       |
| <b>Young bituminous</b> | CO              | 2.21                      | 6.56         | 3.84        | 0.23                          | 1.22*10 <sup>4</sup>          | 107                   | 1.12*10 <sup>9</sup>          | 317                   |
|                         | CO <sub>2</sub> | 2.40                      | 0.57         |             |                               |                               |                       |                               |                       |
| <b>Old Bituminous</b>   | CO              | 0.58                      | 3.22         | 2.07        | 0.14                          | 6.98*10 <sup>4</sup>          | 126                   | 6.25*10 <sup>8</sup>          | 309                   |
|                         | CO <sub>2</sub> | 2.42                      | 0.25         |             |                               |                               |                       |                               |                       |

Notes:

- (a) Oxygen balance is computed as  $(0.5CO+CO_2) / (O_2)_{input}$ , where CO and CO<sub>2</sub> is the total amount produced during TK and TPD (< 1100°C and 1430°C).
- (b) If K0 is set at 10<sup>10</sup> min<sup>-1</sup>, then the recovered E is 219.3 kJ/mol, 228.6 kJ/mol, 227.1 kJ/mol, 228.5 kJ/mol from up to down respectively.
- (c) If K0 is set 10<sup>10</sup> min<sup>-1</sup>, then the recovered E is 352.1kJ/mol, 355.8 kJ/mol, 346.8kJ/mol, 343.8 kJ/mol from up to down respectively.
- (d) If using the equation developed by Redhead<sup>35</sup> listed below where assuming  $V_1$  is 10<sup>10</sup> min<sup>-1</sup>, E will be 239.26 kJ/mol at 725°C and 414.25 kJ/mol at 1430°C.  
can be obtained by the equation to calculate E\* developed by Du et al.<sup>36</sup>

$$E / RT = \ln \frac{v_1 T}{\beta} - 3.64$$

## List of Figure Captions

**Figure 1.** Experimental apparatus.

**Figure 2.** Productions of CO and CO<sub>2</sub> during pyrolysis and oxidation of chars produced at 629°C. CO<sub>2</sub> is the principal product of oxidation. Young chars produce more CO<sub>2</sub> than old chars during oxidation. Young lignite char produces more CO<sub>2</sub> but less CO than bituminous coal chars. The faster decay of oxides from young chars (of both lignite and bituminous coal) suggests higher turnover rates of oxygen on young chars.

**Figure 3.** Productions of CO and CO<sub>2</sub> during pyrolysis and oxidation of chars produced at 1400°C. CO is the main product of combustion at; very little CO<sub>2</sub> is produced from both chars. Lignite chars, young and old, produce more CO than their counterparts derived from bituminous coal. Young lignite char releases more CO than old char, but the CO yields from young and old chars derived from the bituminous coal are comparable. Surface oxides on young chars desorb faster than those on the old chars, and surface oxides on lignite chars desorb faster than those on the bituminous coal chars.

**Figure 4.** TPD spectra of chars pyrolyzed and oxidized at 629°C. Young chars produce much more CO and CO<sub>2</sub>; lignite chars produce more desorption products than bituminous coal chars. CO emissions are highest at three temperature ranges: 685-750°C, 1410-1455°C, and 1700°C. Chars from the bituminous coal seem to have another small peak at 1100°C. Notable CO<sub>2</sub> emission takes place only at about 700°C. The CO peaks produced in the temperature range of 1410-1455°C suggest the existence of stable surface oxides on the basal planes with activation energies above 300 kJ/mol. The large emissions of CO at 1700°C become a focal point in the second part of the current study.

**Figure 5.** TPD spectra of chars pyrolyzed and oxidized at 1400°C. There are no notable CO emissions in the temperature range of 685-750°C implying the unstable nature of these weak surface oxides at 1400°C. Except for the young lignite char, the CO peaks at round around 1430°C are no longer obvious, likely due to the high oxidation temperature.

**Figure 6.** Alumina tube-involved reactions. Trace I illustrates the CO emissions from reaction of 1 g of graphite and alumina U-tube, products may also include aluminum oxycarbides. Trace II illustrates the CO<sub>2</sub> production from reaction of 8000 ppm of CO and alumina tube, such as  $Al_2O_3 + 2CO \rightleftharpoons Al_2O + 2CO_2$ . Trace III represents O<sub>2</sub> production from an empty alumina tube, such as  $Al_2O_3 \rightleftharpoons Al_2O_{(g)} + O_2$ ; highly purified He was used as the carrier this experiment.

**Figure 7.** Reduction of alumina tube with low concentration CO. The stoichiometrically consistent CO<sub>2</sub> increase and CO<sub>2</sub> increase over a wide temperature range supports the postulated reaction  $Al_2O_3 + 2CO \rightleftharpoons Al_2O + 2CO_2$ . CO concentration remains constant initially suggesting relaxation of the mass spectrometer detector is not a problem when CO concentration is reduced. CO concentration continues to decrease during the isothermal period at peak temperature imply the possibility of a progressive pore-enlargement mechanism.

**Figure 8.** Effects of gas residence time on (graphite + alumina) reaction. The U-shaped tube with 500 mg of graphite in its bottom was heated to 1200°C with a heating rate 5°C/min and a He flow rate 100 cc/min. The flow rate was increased to 250 and 500 ml/min at peak temperature. The dependence of flow rate implies kinetically controlled wall reactions.

**Figure 9.** Reactions of SiC tube with 300ppm O<sub>2</sub>. The oxidation of SiC begins at about 650°C. Both CO<sub>2</sub> and CO form initially, and CO is the only oxidation product above 1250°C.

**Figure 10.** Reactions of SiC tube with CO<sub>2</sub>. The straight SiC tube is oxidized to CO. The expectedly high yield of CO at high temperatures is likely the decomposition products of SiO<sub>2</sub> from earlier experiments.

**Figure 11.** Removal of SiO<sub>2(s)</sub> scale on SiC tube by heat treatment. After oxidation experiments by O<sub>2</sub> and CO<sub>2</sub>, the straight oxidized SiC tube is restored for TPD by heating to 1650°C at 5°C/min with a flow of 80 ml/min He. The tube was kept at 1650°C until CO concentration decreased to the baseline. SiO<sub>2(s)</sub> reacts with SiC and converted to SiO<sub>(g)</sub>, Si<sub>(s)</sub>, C<sub>(s)</sub>, see text for more details.

**Figure 12.** Emissions from the (SiC tube + rod + foam + wool). The SiC tube with 0.65 gm of ceramic wool inside was heated with flowing He. A small amount of CO<sub>2</sub> was detected around 450°C. The large and steady emission of CO at high temperatures is likely the reaction product of SiO<sub>2</sub> in the wool with SiC. Thus, the ceramic wool is not suitable to high temperature desorption experiments in a SiC tube.

**Figure 13.** Heat treatment of SiC rod, foam and beads for two consecutive times. Since the rod and foam have been used in the previous TPD experiments with chars and ceramic wool, the CO yield during treatment may be due to the reaction of SiC and SiO<sub>2</sub> scale. It may be caused by impurities in the beads. These results suggest tube can be restored for TPD experiments after heat treatment.

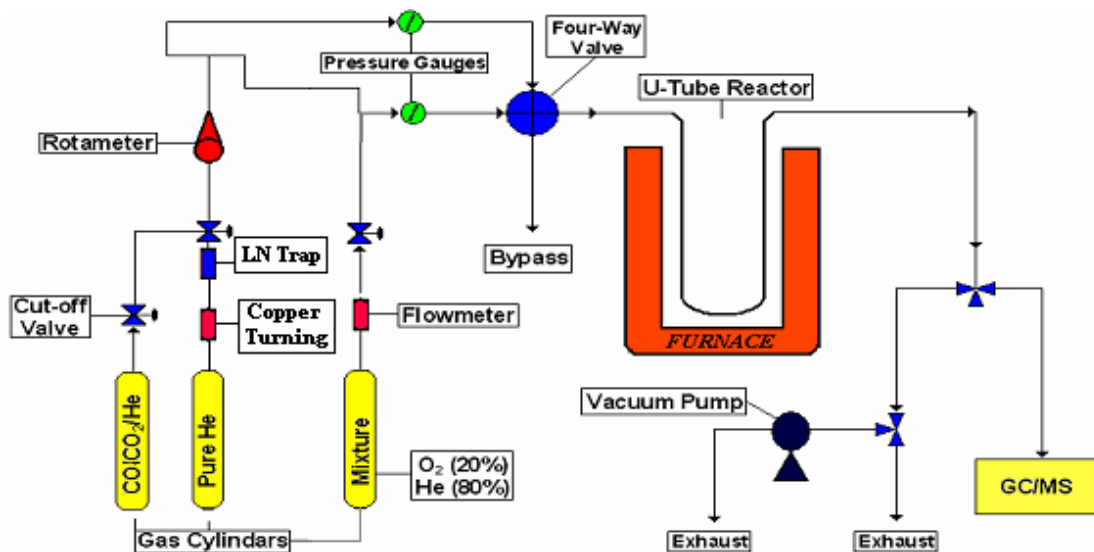


**Figure 1.** Experimental apparatus.

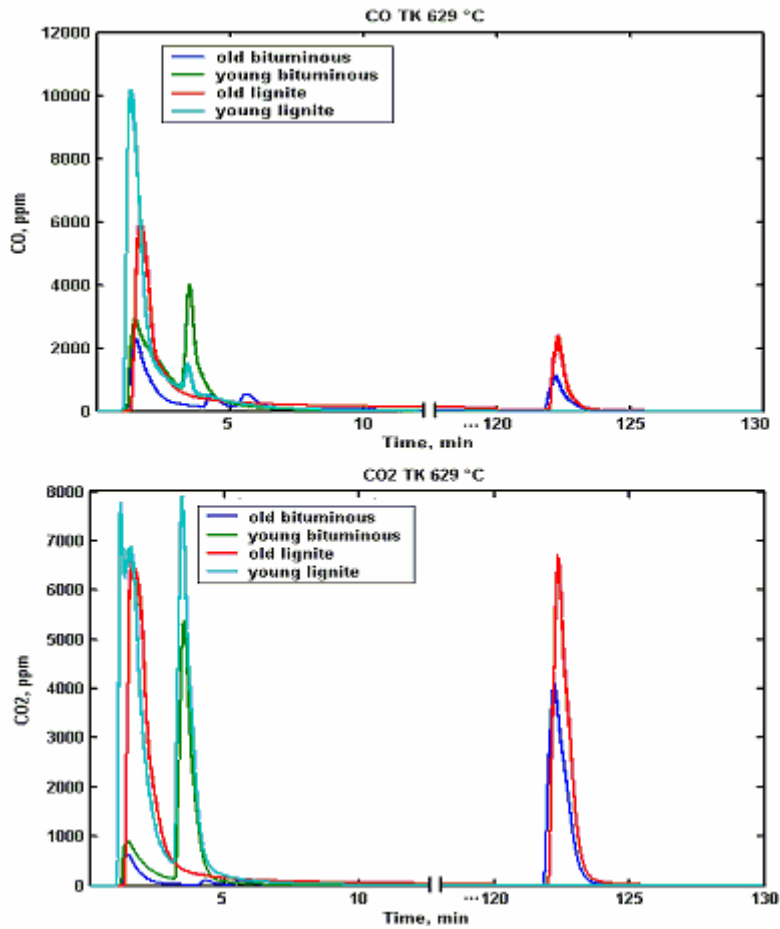


**Figure 2.** Productions of CO and CO<sub>2</sub> during pyrolysis and oxidation of chars produced at 629°C. CO<sub>2</sub> is the principal product of oxidation. Young chars produce more CO<sub>2</sub> than old chars during oxidation. Young lignite char produces more CO<sub>2</sub> but less CO than bituminous coal chars. The faster decay of oxides from young chars (of both lignite and bituminous coal) suggests higher turnover rates of oxygen on young chars.

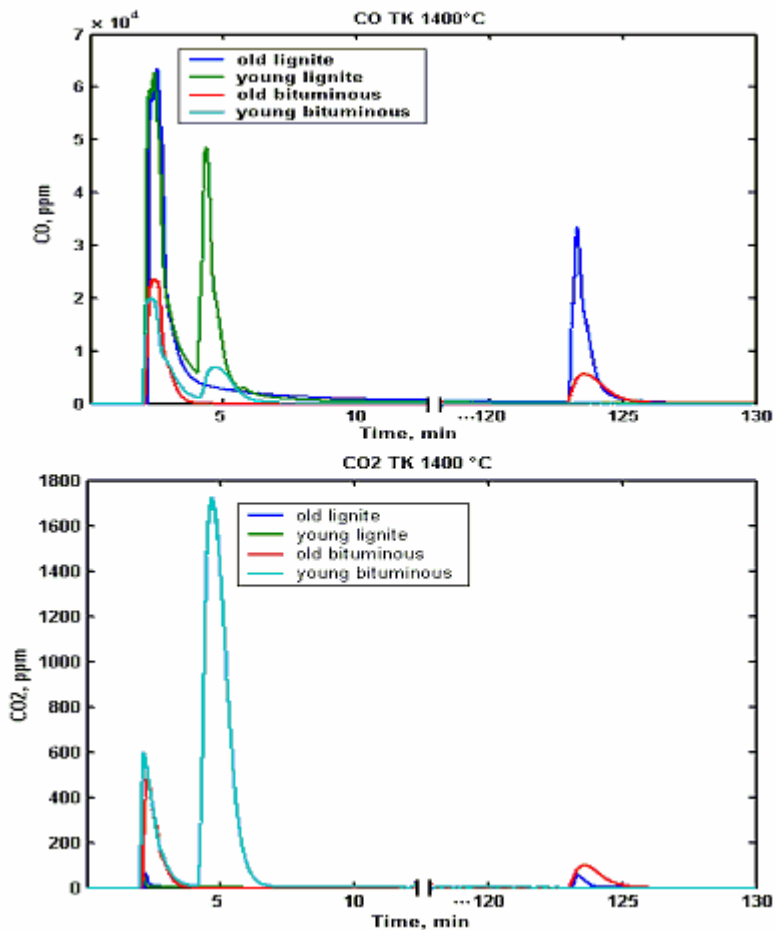


**Figure 3.** Productions of CO and CO<sub>2</sub> during pyrolysis and oxidation of chars produced at 1400°C. CO is the main product of combustion at; very little CO<sub>2</sub> is produced from both chars. Lignite chars, young and old, produce more CO than their counterparts derived form bituminous coal. Young lignite char releases more CO than old char, but the CO yields from young and old chars derived from the bituminous coal are comparable. Surface oxides on young chars desorb faster than those on the old chars, and surface oxides on lignite chars desorb faster than those on the bituminous coal chars.

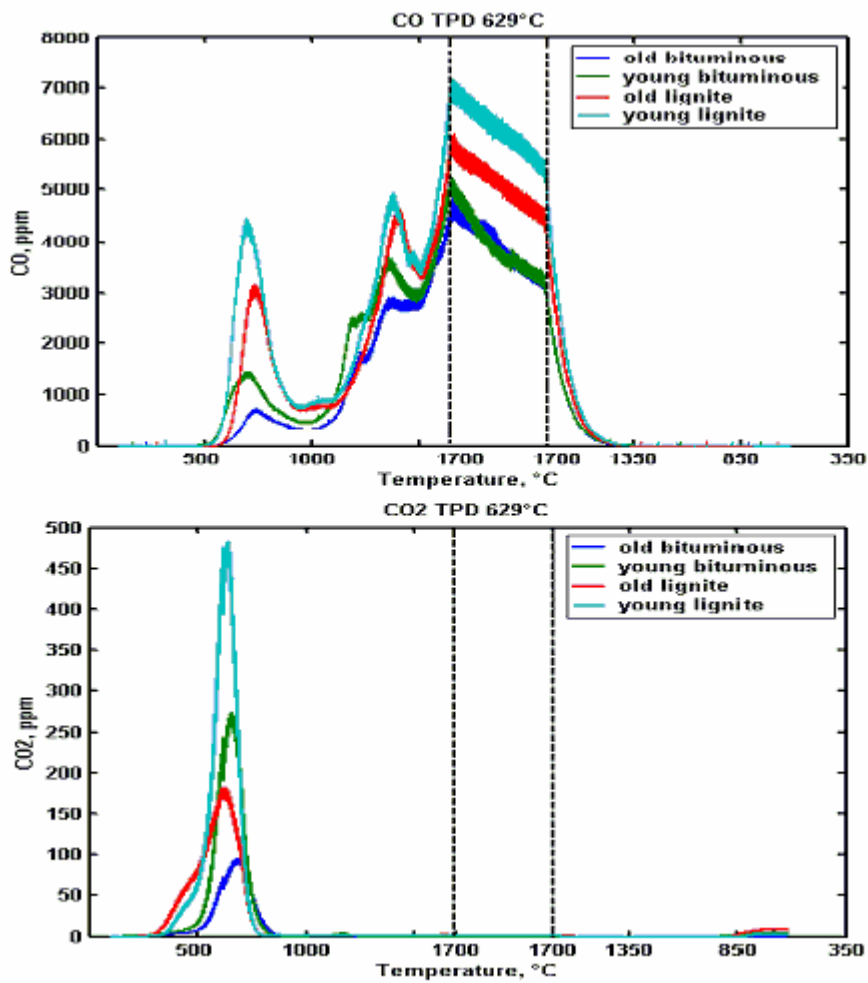


**Figure 4.** TPD spectra of chars pyrolyzed and oxidized at 629°C. Young chars produce much more CO and CO<sub>2</sub>; lignite chars produce more desorption products than bituminous coal chars. CO emissions are highest at three temperature ranges: 685-750°C, 1410-1455°C, and 1700°C. Chars from the bituminous coal seem to have another small peak at 1100°C. Notable CO<sub>2</sub> emission takes place only at about 700°C. The CO peaks produced in the temperature range of 1410-1455°C suggest the existence of stable surface oxides on the basal planes with activation energies above 300 kJ/mol. The large emissions of CO at 1700°C become a focal point in the second part of the current study.

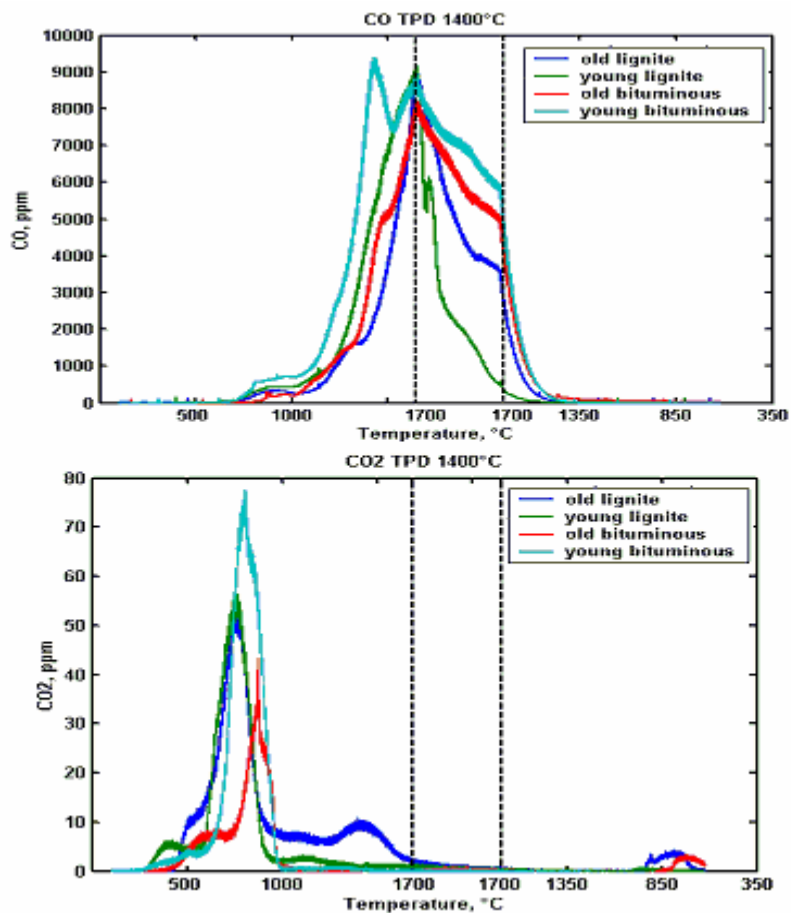


**Figure 5.** TPD spectra of chars pyrolyzed and oxidized at 1400°C. There are no notable CO emissions in the temperature range of 685-750°C implying the unstable nature of these weak surface oxides at 1400°C. Except for the young lignite char, the CO peaks at round around 1430°C are no longer obvious, likely due to the high oxidation temperature.

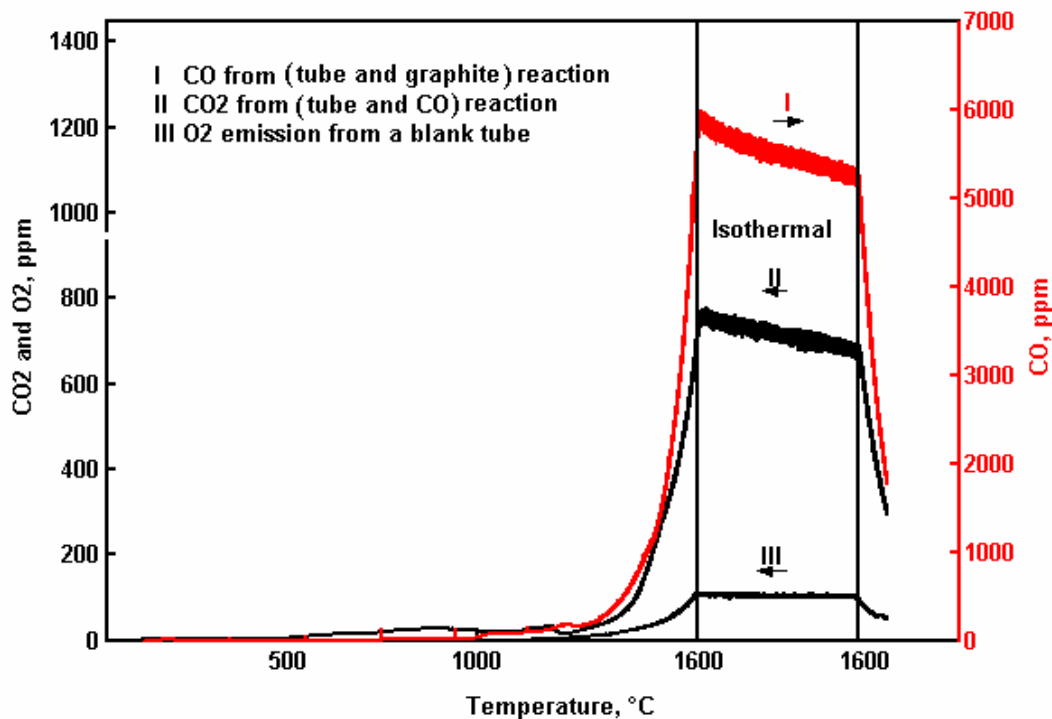


**Figure 6.** Alumina tube-involved reactions. Trace I illustrates the CO emissions from reaction of 1 g of graphite and alumina U-tube, products may also include aluminum oxycarbides. Trace II illustrates the CO<sub>2</sub> production from reaction of 8000 ppm of CO and alumina tube, such as  $Al_2O_3 + 2CO \rightleftharpoons Al_2O + 2CO_2$ . Trace III represents O<sub>2</sub> production from an empty alumina tube, such as  $Al_2O_3 \rightleftharpoons Al_2O_{(g)} + O_2$ ; highly purified He was used as the carrier this experiment.

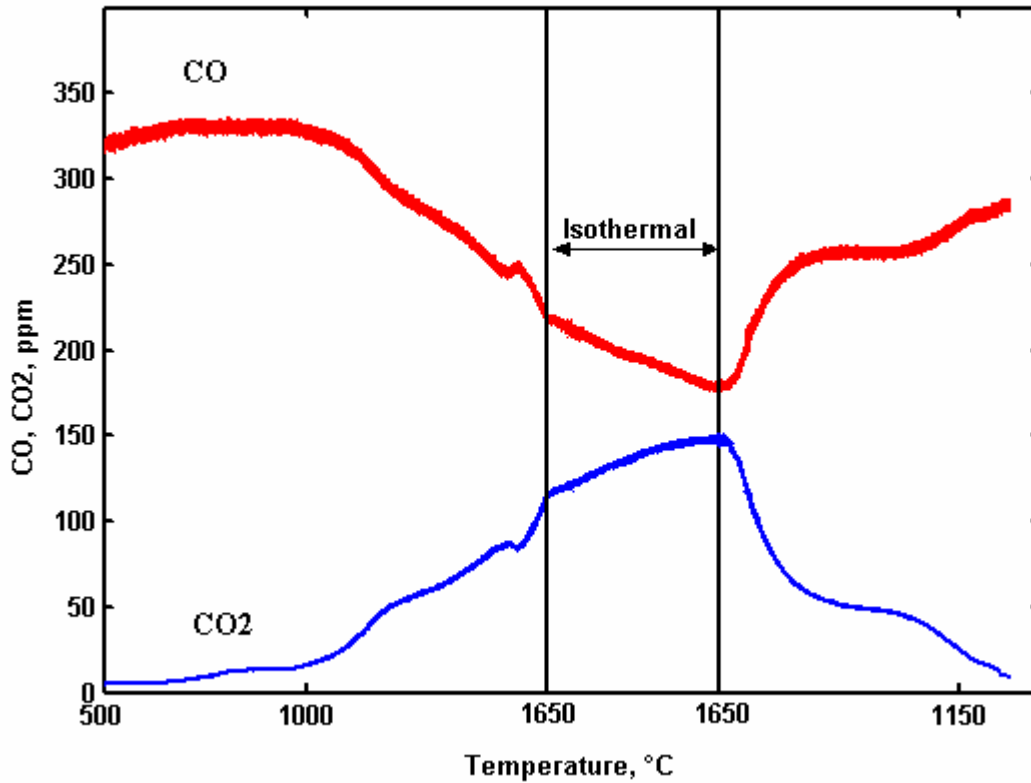


**Figure 7.** Reduction of alumina tube with low concentration CO. The stoichiometrically consistent CO<sub>2</sub> increase and CO<sub>2</sub> increase over a wide temperature range supports the postulated reaction  $Al_2O_3 + 2CO \rightleftharpoons Al_2O + 2CO_2$ . CO concentration remains constant initially suggesting relaxation of the mass spectrometer detector is not a problem when CO concentration is reduced. CO concentration continues to decrease during the isothermal period at peak temperature imply the possibility of a progressive pore-enlargement mechanism.

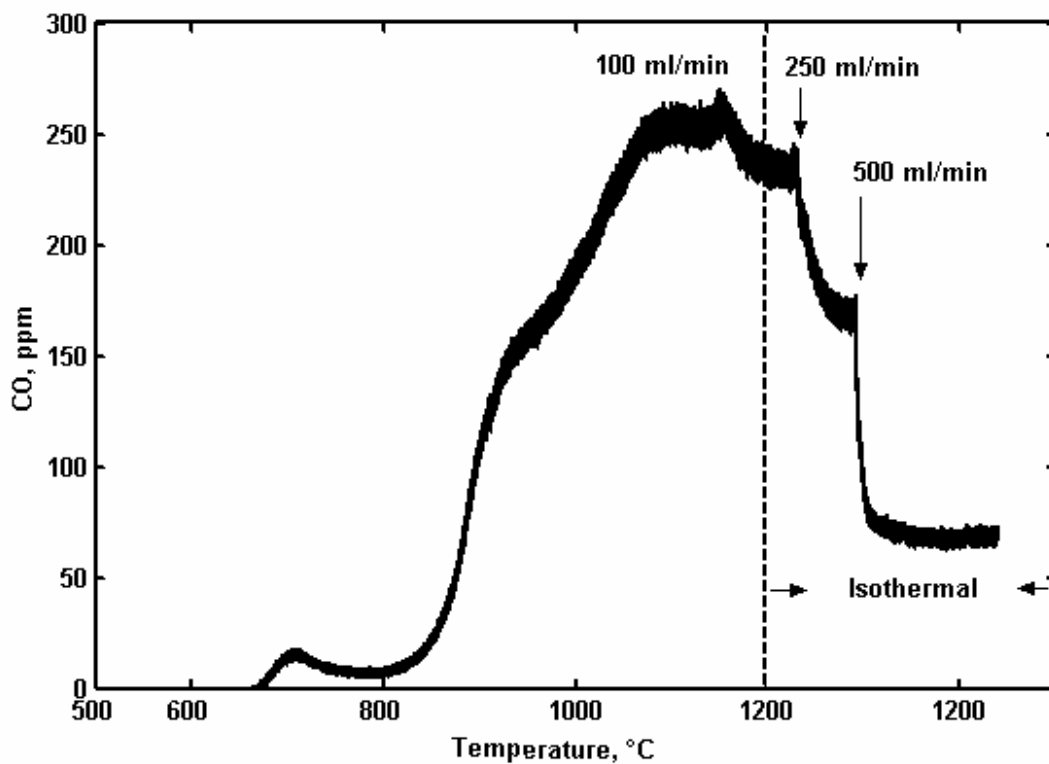


**Figure 8.** Effects of gas residence time on (graphite + alumina) reaction. The U-shaped tube with 500 mg of graphite in its bottom was heated to 1200°C with a heating rate 5°C/min and a He flow rate 100 cc/min. The flow rate was increased to 250 and 500 ml/min at peak temperature. The dependence of flow rate implies kinetically controlled wall reactions.

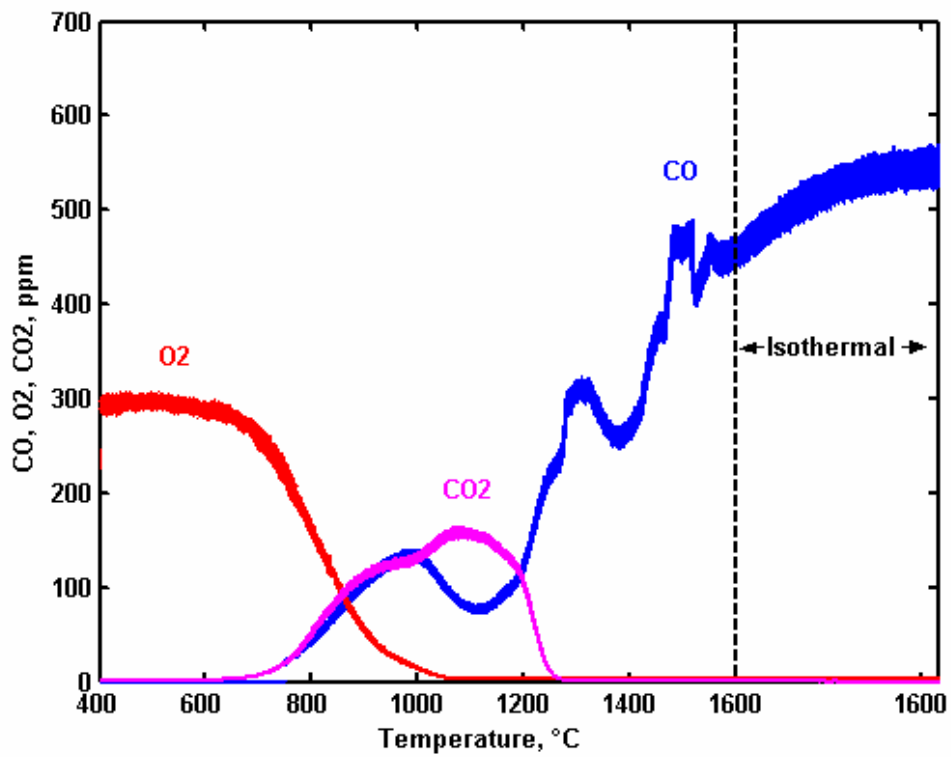


**Figure 9.** Reactions of SiC tube with 300ppm O<sub>2</sub>. The oxidation of SiC begins at about 650°C. Both CO<sub>2</sub> and CO form initially, and CO is the only oxidation product above 1250°C.

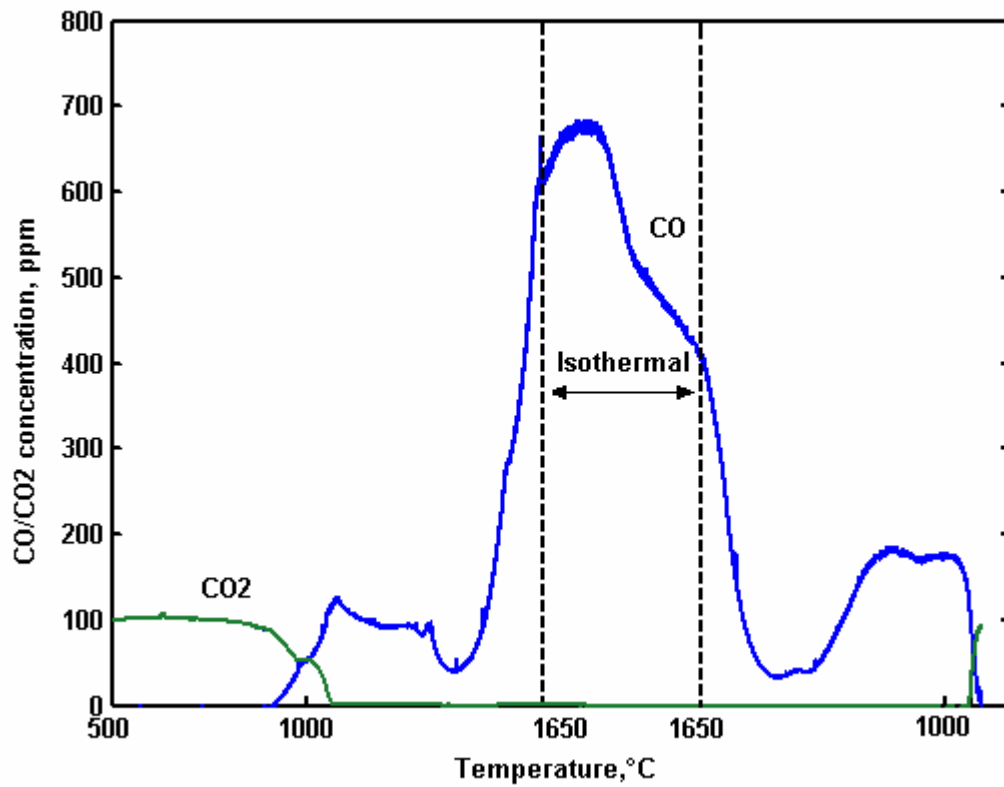


**Figure 10.** Reactions of SiC tube with CO<sub>2</sub>. The straight SiC tube is oxidized to CO. The expectedly high yield of CO at high temperatures is likely the decomposition products of SiO<sub>2</sub> from earlier experiments.

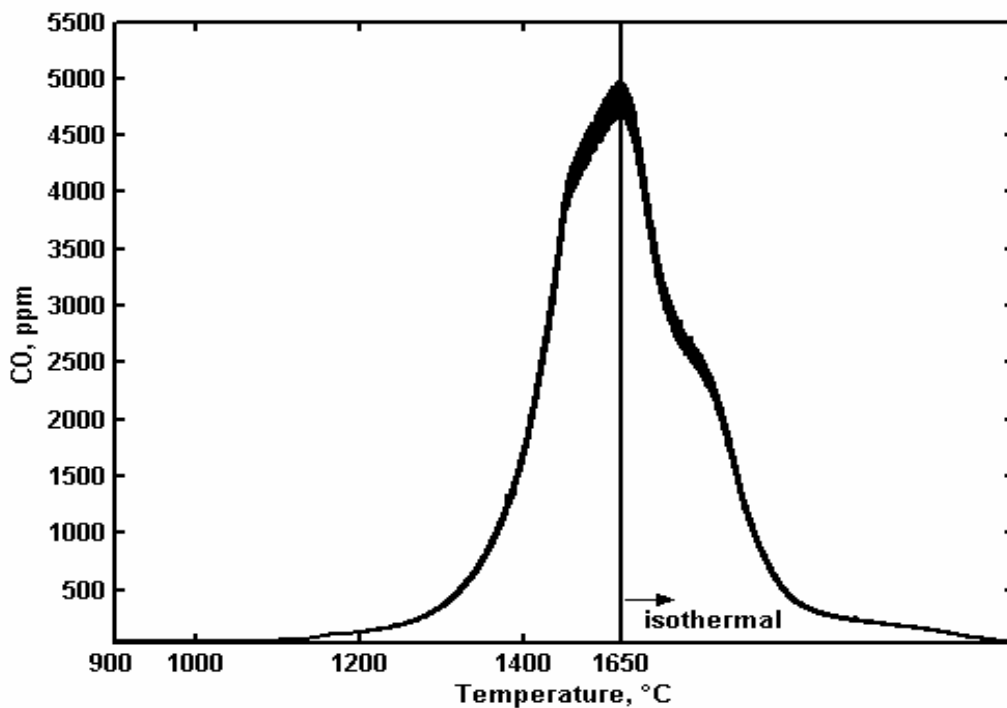


**Figure 11.** Removal of  $\text{SiO}_{2(s)}$  scale on SiC tube by heat treatment. After oxidation experiments by  $\text{O}_2$  and  $\text{CO}_2$ , the straight oxidized SiC tube is restored for TPD by heating to  $1650^\circ\text{C}$  at  $5^\circ\text{C}/\text{min}$  with a flow of  $80\text{ ml}/\text{min}$  He. The tube was kept at  $1650^\circ\text{C}$  until CO concentration decreased to the baseline.  $\text{SiO}_{2(s)}$  reacts with SiC and converted to  $\text{SiO}_{(g)}$ ,  $\text{Si}_{(s)}$ ,  $\text{C}_{(s)}$ , see text for more details.

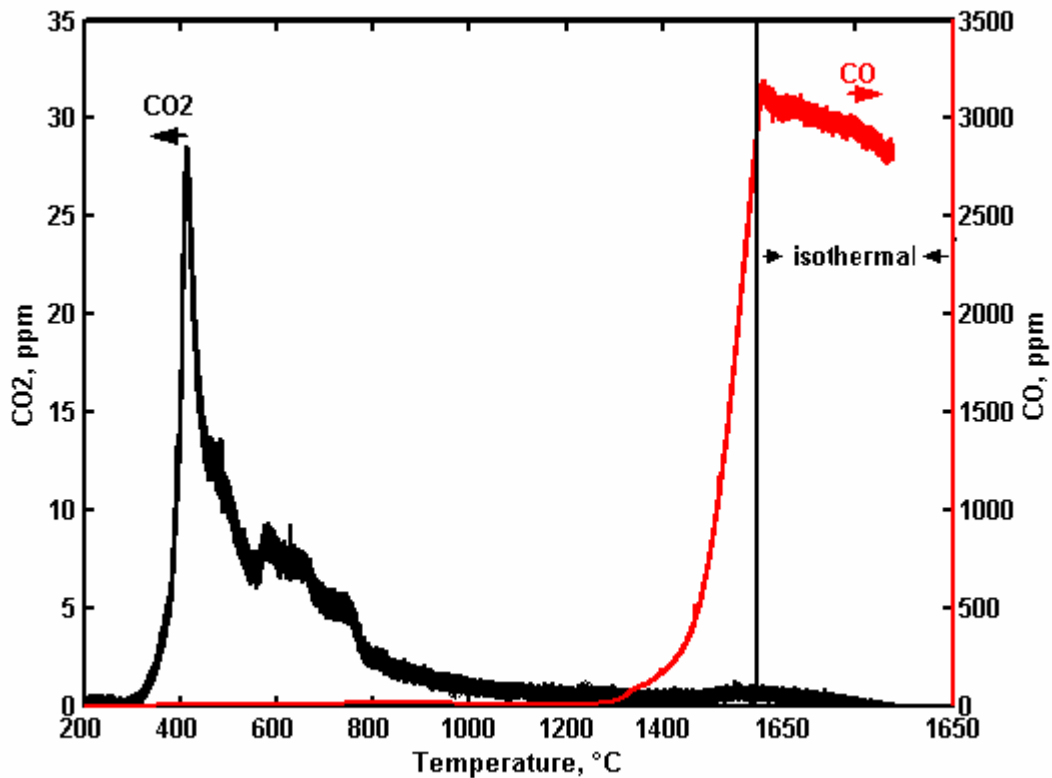


**Figure 12.** Emissions from the (SiC tube + rod + foam + wool). The SiC tube with 0.65 gm of ceramic wool inside was heated with flowing He. A small amount of CO<sub>2</sub> was detected around 450°C. The large and steady emission of CO at high temperatures is likely the reaction product of SiO<sub>2</sub> in the wool with SiC. Thus, the ceramic wool is not suitable to high temperature desorption experiments in a SiC tube.

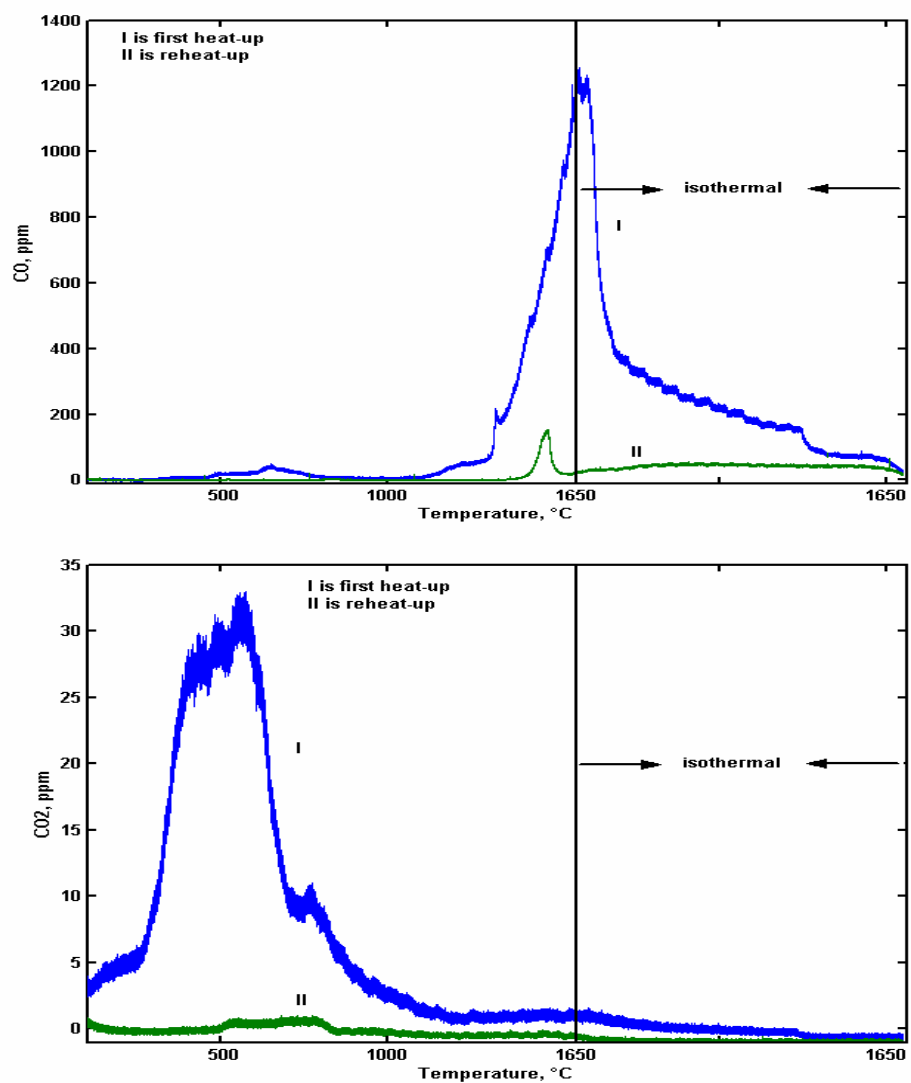


**Figure 13.** Heat treatment of SiC rod, foam and beads for two consecutive times. Since the rod and foam have been used in the previous TPD experiments with chars and ceramic wool, the CO yield during treatment may be due to the reaction of SiC and SiO<sub>2</sub> scale. It may be caused by impurities in the beads. These results suggest tube can be restored for TPD experiments after heat treatment.